# NTNU
Kunnskap for en bedre verden

# Nano-enabled polymers as embedded sensing electrodes in fibre-reinforced polymer composites

Morten M. Dahl
Vegar S. Brøndbo

Gradering: Åpen

◘ **NTNU**
**Institutt for vareproduksjon**
**og byggteknikk**

| Oppgavens tittel:<br>Nano-enabled polymers as embedded sensing electrodes in fibre-reinforced polymer composites | Dato:       17.05.19<br><br>Antall sider:   33 | | |
| --- | --- | --- | --- |
| | Masteroppgave: | Bacheloroppgave: | X |
| Navn:<br>Morten M. Dahl, Vegar S. Brøndbo | | | |
| Veileder:<br>Sotirios Grammatikos | | | |
| Eventuelle eksterne faglige kontakter/ veiledere:<br>Harald B. Jøsendal | | | |

Sammendrag:
Polyuretan ble kombinert med nanoadditivene grafitt og karbon nanorør for å skape en elektrisk ledende elastomer, som videre ble implementert i en epoxy-karbonfiber kompositt for å gjøre bruken av karbonfiber-kompositter som strekksensor mulig.

For å sette metoden på prøve ble det utført materialtester for å avgjøre mekaniske og elektriske materialegenskaper hvor den beste kombinasjonen ble avgjort til å være 3 vekt% karbon nanorør med aceton som løsemiddel.

Bindingsstyken mellom epoxy og polyuretan ble testet ved å lage prøvestaver som forbinder det fysiske grensesnittet mellom de to materialene. De to bestanddelene ble kombinert i forskjellig tidsintervall for å avgjøre om herdetilstanden til bestanddelene avgjorde styrken på forbindelsen. Det ble konkludert med at bindestyrken øker hvis de to fysiske grensesnittene mellom bestanddelene blandes, i forhold til de ublandede grensesnittene hvor overflateruheten har den største innvirkningen.

Det samlede systemet bestående av en karbonfiber kompositt med påsatte polyuretan-elektroder ble satt på prøve ved å utføre last-/avlastningstesting. Resultatet fra denne testen konkluderer at det er en betydelig endring av elektrisk ledeevne under statisk testing, og at denne metoden for å introdusere ledere kan være en mulig skalerbar modell for bruk i industrien.

Stikkord:

| Kompositt |
| --- |
| Strekksensor |
| Nanoadditiver |
| Polyuretan |

*Morten M. Dahl* (signature)

Morten M. Dahl

*Vegar Brøn* (signature)

Vegar S. Brøndbo

# Forord

Oppgaven setter på prøve en metode for å introdusere polyuretan-elektroder i en epoxy-karbonfiber kompositt for å muliggjøre blant annet bruken av kompositkonstruksjonen som strekksensor.

For å kunne bruke polyuretan som elektroder må nanoadditiver tilsettes grunnet at materialet er elektrisk isolativt. Materialene brukt for å skape ledeevne i polyuretanen er grafitt og karbon nanorør. Forskjellige konsentrasjoner av nanoadditiver i polyuretan blir så satt på prøve for å finne den mest egnede blandingen.

Dette evauleres ved å gjennomføre mekaniske og elektriske materialtester av elektrodene, teste forbindelsen mellom epoxy og polyuretan, og til slutt å gjennomføre last-/avlastningstesting hvor kompositten fungerer som en strekksensor.

Denne oppgaven er en bacheloroppgave skrevet av studenter ved maskiningeniørlinjen på NTNU i Gjøvik. Oppgaven er utstedt av Prof. Sotirios Grammatikos, og arbeidet har blitt utført på ASEM laboratoriet i Gjøvik.

# Abstract

This paper explores a method for introducing polyurethane (PUR) electrodes into a carbon fibre reinforced polymer (CFRP) composite to enable the use of the composite structure as a strain sensor, among other uses.

To be able to use polyurethane as electrodes, nanoadditives is added due to the high electrically insulating nature of the material. The materials used to create conductivity in the polyurethane are graphite and multi-walled carbon nanotubes (MWCNTs). Various concentrations of nanoadditives in PUR are then tested to find the most suitable properties for this application.

This is done by performing mechanical and electrical material tests of the electrodes, testing the adhesion capabilities between epoxy and polyurethane and carrying out load-unload testing where the composite acts as a strain sensor.

This paper is a bachelor thesis written by students in the mechanical engineering study at NTNU in Gjøvik. The thesis was issued by Prof. Sotirios Grammatikos, and the work has been carried out at the ASEM laboratory in Gjøvik.

# Table of Contents

# List of Figures

# List of Tables

# List of Terms

*Table 1: List of Terms*

| Term | Explanation |
| --- | --- |
| CFRP | Carbon fibre reinforced polymer. |
| (MW)CNTs | (Multi-walled) Carbon Nanotubes. Grapite layer(s) rolled into tubes. |
| Delamination | Mode of failure where a material fractures in to layers |
| Matrix | The continuous phase of a composite which transfers stress to reinforcing fibres, as well as protecting the fibres from the environment. |
| Nanoadditive | Nanoscaled solid particles used as additives |
| FDM printing | Fused deposition modelingn |
| Graphite (G) | Multiple layers of graphene. |
| PLA | Polylactic acid. A thermoplastic commonly used in additive manufacturing using FDM printers. |
| PUR | Polyurethane. A versatile elastomer with many applications. |
| Soncation | The use of sound energy to agitate and suspend particles in a medium. |
| Shore | Scale for measuring hardness of a material |
| THF | Tetrahydrofuran. A solvent commonly used in industrial applications. |

x

# 1 Introduction

Modern use of carbon fibre-reinforced polymer (CFRP) can include multifuncional use of the composite. This involves utilizing abilities such as strain sensing, self healing, self heating, energy harvesing and many more, at the same time as being a structural element (Narayana and Burela 2018). This multifunctional use has seen a large amount of research in the last few years, but has not yet been widely applied in any field of engineering. To detect strain or delaminations, electrodes are inserted into the composite and the change in resistance over time is monitored (Wang and D.D.L. Chung 1997; Karl and Baron 1989; Wang, Fu, and Deborah Chung 1999). The change in resistance is caused by the piezoresistive effect. This effect causes the resistance of a material to increase when mechanical strain is applied (Xi and D.D.L. Chung 2019).

So far, many studies have used either copper, gold or silver as electrodes in their composites (Yao, Hawkins, and Falzon 2018; Fukuda 1994; Joo et al. 2017). These electrodes have to either be connected to the fibre endings, or to the surface by removing matrix material in the connection area to provide a sufficient interfacial connection (Joo et al. 2017). Due to metals being less ductile than the matrix material, the interfacial bond between epoxy and metal is prone to failure over time (Grammatikos and A.S. Paipetis 2012). As these electrodes are integrated in the structure of the composite, their weakening is unacceptable due to their installation and adhesion directly to the load-bearing fibres.

In this thesis we have investigated the composition of electrodes that can be used to counteract these effects. A CFRP with an epoxy matrix, combined with nanoenhanced polyurethane (PUR) as an electrode was used. PUR is known for it's great adhesion properties, as well as abrasion, weathering and electrical resistance (Saunders and Frisch 1964; Urbanski et al. 1977; Fried 1997) making them ideal for many different applications. To provide electrical conductivity to an otherwise isolating PUR, CNTs and graphite at different concentrations were added and tested to find the most optimal combination between
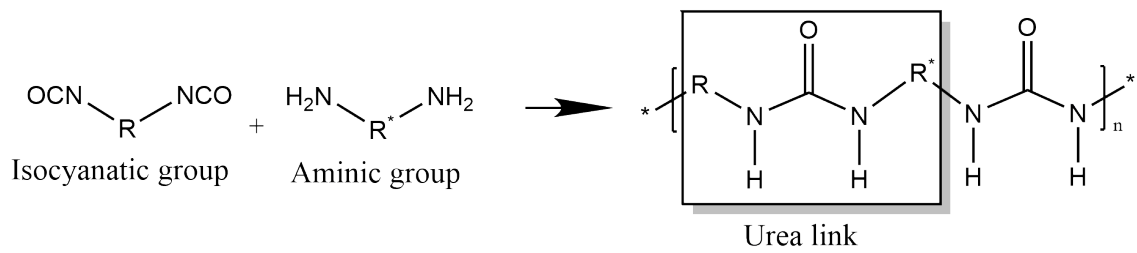
*Figure 1: Chemical reaction between aminic groups in epoxy hardener and isocyanatic groups in PUR hardener.*

conductivity and strength. During the curing of PUR and epoxy together, isocyanate and aminic groups react and form an urea link (figure 1). This provides a chemical bonding increasing the interfacial strength (Juss and Mertiny 2009). The high interfacial strength could prevent the influence of surface resistance during mechanical loading and provide high mechanical interlocking and a stable interface between the electrodes and the composite. This also allows for the electrode-metal connection to exist outside of the dynamic system. The electrodes stretch from the connection to the fibre surface to the outside of the composite, having one part attached to the dynamic system and the other part outside. The outside part of the electrode which is connected to wires will not be exposed to the same strain as the connected part, and therefore increase its lifetime. To evaulate the bonding between PUR and epoxy, adhesion testing with different hardening times of the PUR, as well as mixing of the interface was conducted. The change in mechanical properties of PUR with nanoadditives was determined by tensile testing, and the change in electrical properties was determined by relative resistance measurments. To evaluate the use as electrodes in a CFRP, load-unload testing was conducted. The change of interface between PUR and the CFRP was evaluated by investigating any interfacial changes using ultrasonic imaging.

2

# 2 Method

## 2.1 Materials

Multi-walled carbon nanotubes (MWCNTs) were purchased from NANOCYL® under the trademark NC7000$^{TM}$ with an average length and diameter of $1.5\,\mu$m and $9.5\,$nm respectively. The graphite particles that is used have an average diameter of 200 mesh ($74\,\mu m$) and is given the denomination "G" in this thesis. Gurit SP 106 epoxy resin and slow hardener was employed as the polymer matrix of the studied CFRP. The mixing ratio of the epoxy resin to hardener used in all samples is 100:18 by weight. 3K 2x2 twill weave 200g carbon fibre manufactured by Mitsubishi Rayon under the trademark Pyrofil$^{TM}$ was used as reinforcement. The polyurethane contains polyol, isocyanate (MDI modified with tripropylene glycol) and 1,4-butanediol (XLB), all produced by Covestro. Anhydrous and inhibitor free THF used as solvent is produced by Honeywell. The acetone also used as solvent was purchased from Biltema Norge AS, and is also free of inhibitors.

## 2.2 Preparation of samples

### 2.2.1 Preparation of adhesion testing samples

For evaluating the adhesion strength between the PUR electrode and epoxy, two sets of samples were prepared:

- Non-mixed interface with four different curing times of PUR

- Manually mixed interface between PUR and epoxy

A two-part mould depicted in figure 2 was printed on a Prusa i3 MK2 FDM printer using polylactic acid (PLA) material, designed to create three double-thickness 1A dogbone samples. The moulds were set with Acmosil 36-4672 release agent and filled halfway with PUR using a syringe. The PUR was set to cure at different time intervals, 0, 1, 3 and
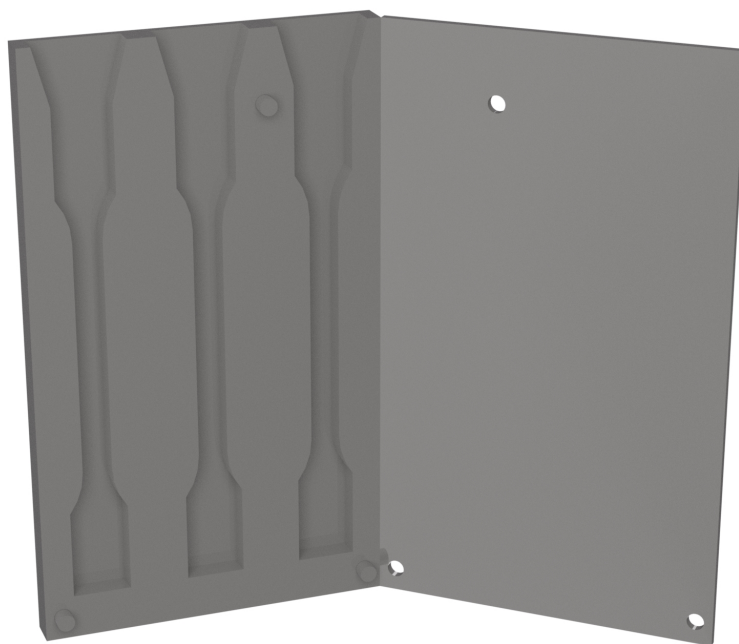
*Figure 2: Two-part mould for producing adhesion testing samples.*

24 h, and epoxy was added on top of the PUR. For the mixed-interface samples, the two-part mould was split and the mould was filled from both sides simultaniously with a PLA splitter in the middle of the mould. When both sides were filled, the splitter was removed and the interface was mixed together manually using a thin metallic tip. The moulds were then set to cure for 12 h at $22 \pm 3°C$, $30 \pm 5\%$ RH. The samples were demoulded and put in an oven at $60°C$ for another 48 h for post-curing.

### 2.2.2 Preparation of the polyurethane electrodes

The chosen nanoadditive is added to either THF or acetone solvent based on the sample to be tested. The mix of solvent and nanoadditive is then added to a Hielscher UP400St sonicator and is sonicated for an effective 30 min at 15-60W with a frequency of 24kHz

4

to achieve a fine dispersion that increases the conductivity of the final polymer electrode (Pokharel et al. 2019). Polyol was then added and the sonication was resumed for another 30 min to mix the polyol into solution. The solvent was then distilled off using a hotplate set to a surface temperature of around $100\,°C$ for 1 to 2 h. After cooling to around $30\,°C$, XLB was added to the polyol-nanomodified solution and manualy mixed for 15 min. The finished pre-polymer was then ready to be reacted with isocyanate to begin the hardening process. The production method is depicted in the flowchart found in figure 4, and the complete list of samples made can be found in table 2. The samples were then added to a mould depicted in figure 5a, with dimensions given in figure 3. For the samples to be used as electrodes in the CFRP-PUR composite, the first layer of carbon fibre was added. For the samples to be used to determine electrical and mechanical properties, the PUR composite was left for 24 h to cure. The samples were then post-cured at $60\,°C$ for 48 h. The hardness of the reference sample of PUR without any additives or solvents is approximately 65 shore A.
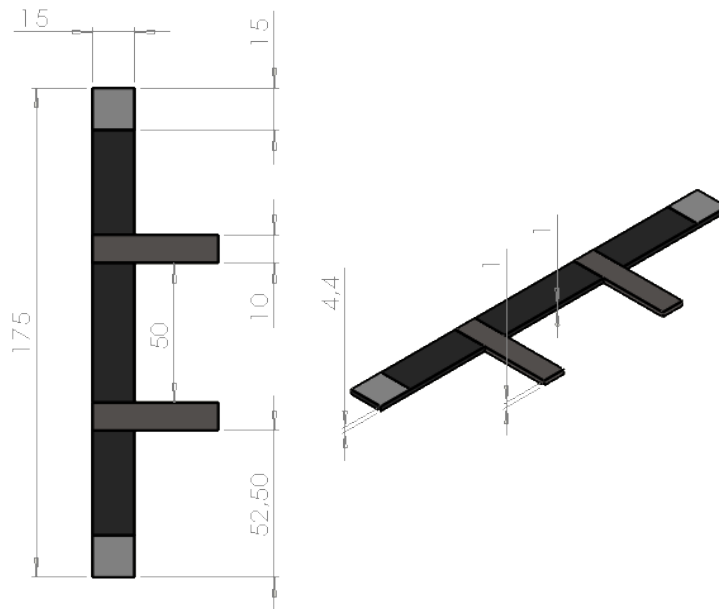


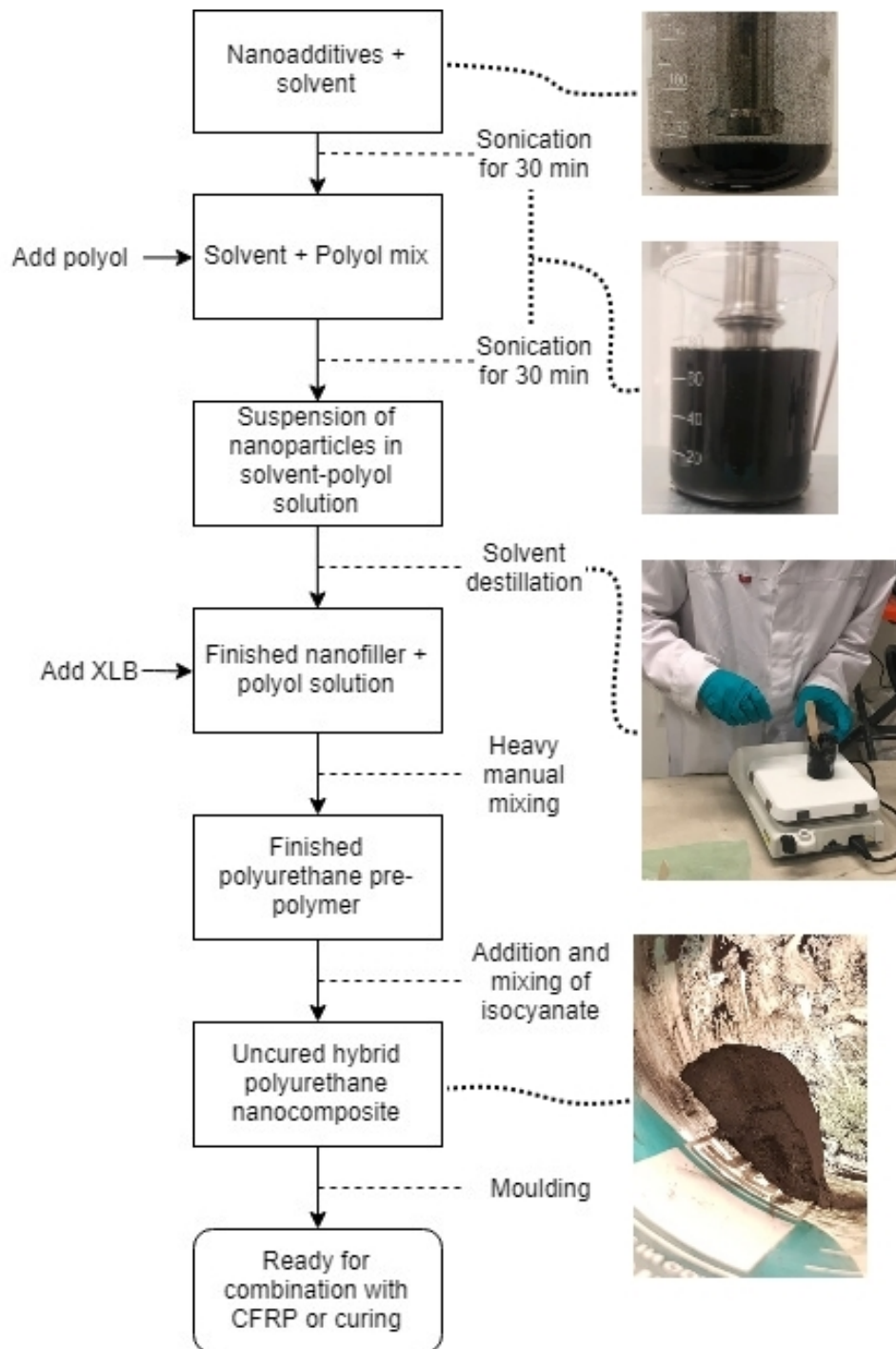*Figure 3: Visualisation of the CFRP-PUR composite. All dimensions are given in millimetres.*

*Figure 4: Production process of the polyurethane nanocomposite.*

### 2.2.3 Preparation of tensile testing samples

To determine the tensile strength of the PUR electrodes at different nanofiller concentration, the same samples used for determination of electrical properties was used. This ensures accurate correlation between the mechanical and electrical properties for the specific material composition.

### 2.2.4 Preparation of CFRP-PUR composite

To create the CFRP-PUR composite to be used for strain sensing, two moulds were made on the FDM printer using PLA (figure 5). The first mould, mould A, is used to manufacture electrodes as explained in section 2.2.2. Mould A is removed and mould B is applied. The first layer of carbon fibre is then added on top of the PUR electrodes, and light pressure is given on the fibres to ensure good bonding between the fibres and the electrodes (as shown in figure 6). Epoxy is then added to the first layer with light agitation in the areas of the PUR electrodes to encourage wetting of the fibres, as well as light mixing and bonding between the PUR and epoxy. The remaining three layers of carbon fibres are then wetted on their own and applied on top of the first layer. A lid was then applied on top of the stack and weights were added to get rid of excess epoxy. The CFRP is set to cure under pressure from the weights for 12 h. The CFRP-PUR composite is then demoulded and post-cured in a 60 °C oven for 48 h.

The finished stack consisting of 4 plies of carbon fibre (figure 5) is then cut into four samples. End-tabs made from 8-ply [0/90] glass fibre reinforced polymer composite is cut to size and sanded. The ends of the CFRP samples are sanded, washed with acetone and dried before applying Crestabond M7-05 MMA adhesive. The tabs were then bonded to the samples under pressure from clamps. The adhesive used for the end-tabs was cured for 12 h in room temperature, then another 12 h at 60 °C.
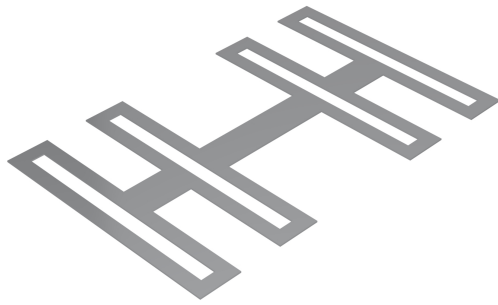
*(a) Mould A*
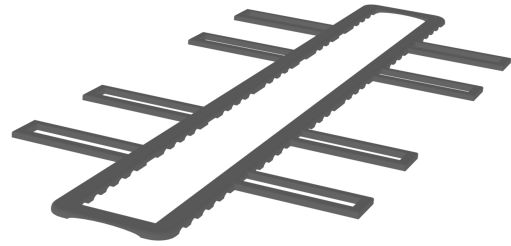
*(b) Mould B*
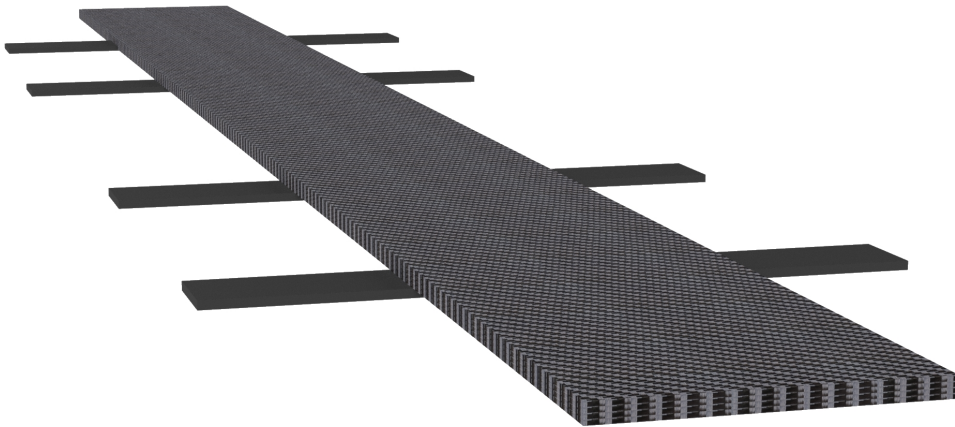


*(c) Finished composite*

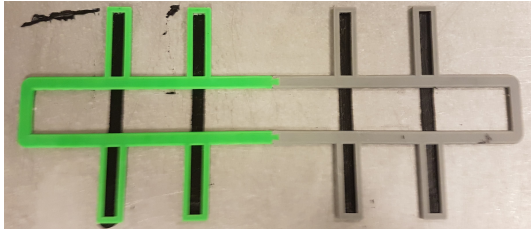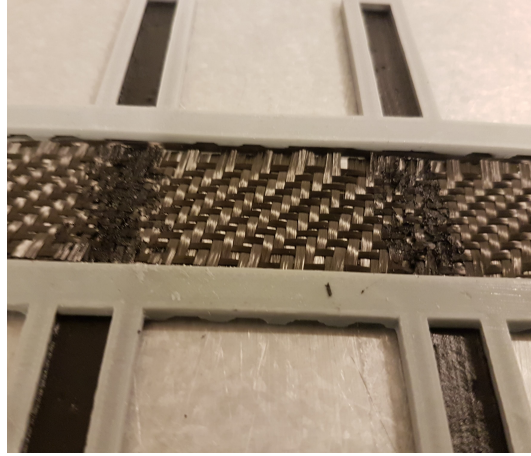*Figure 5: Moulds used in the production of composite samples.*

*(a) Mould B mounted.*



*(b) Carbon fibres added on top of the elec-trodes.*

*Figure 6: Mould B before and after the first layer of carbon fibre is applied.*



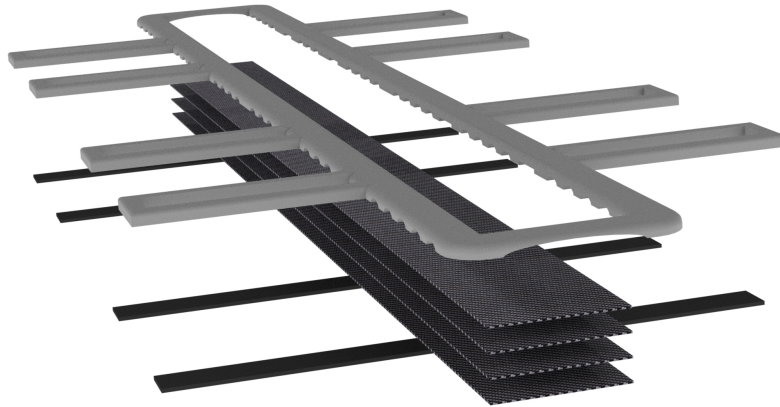*Figure 7: Exploded view of the mould and fibre stacking method for the CFRP-PUR composite*

## 2.3   Experimental

### 2.3.1   Adhesion testing

The samples were tested in a tensile testing machine (Instron 5966 electromechanical tensile testing machine with pneumatic grips) at a rate of 10 mm/min.

### 2.3.2   Measuring mechanical properties

The samples were tested in the tensile testing machine set to a testing rate of 50 mm/min. An overview of the samples tested can be found in table 2.

### 2.3.3   Measuring electrical properties

Wires were connected to the PUR electrodes using a crocodile clip. Aluminium tape was applied on the electrodes to increase the connection area. The wires were then connected in series to a Fluke 45 multimeter and a Thurbly PL320 power supply to record resistance (see figure 8). The voltage applied varied from 25 V to 30 V, and the resulting electric current was recorded. From this the resulting resistance was calculated, and by using the area of the electrodes and length between the connection areas the resistivity ($\rho$) was calculated using the formula:

$$\rho = \frac{R \cdot A}{\ell} \tag{1}$$

Where $R$ is the electrical resistance, $A$ is the area of the cross section and $\ell$ is the length between the connected areas.

### 2.3.4   Load-unload testing

To determine the ability to use the CFRP-PUR composite as an strain gauge, the tensile testing machine was used together with the power supply and the multimeter shown in figure 9. This setup makes it possible to expose the composite sample to stress while monitoring the change of resistance.

10

*Table 2: Overview of all the PUR electrode samples and test methods they are part of.*

| Denomination | Solvent used | Nanofiller type | Filler wt.% | Mech | Electrical |
|---|---|---|---|---|---|
| Ref | None | - | 0 | X | X |
| Ref acetone | Acetone | - | 0 | X | X |
| Ref THF | THF | - | 0 | X | X |
| 0.5CNT Acetone | Acetone | MWCNTs | 0.5 | X | - |
| 1CNT Acetone | Acetone | MWCNTs | 1 | X | X |
| 1CNT THF | THF | MWCNTs | 1 | X | X |
| 1G THF | THF | Graphite | 1 | X | - |
| 3CNT Acetone | Acetone | MWCNTs | 3 | X | X |
| 3CNT THF | THF | MWCNTs | 3 | X | X |
| 3CNT None | None | MWCNTs | 3 | X | X |
| 5CNT Acetone | Acetone | MWCNTs | 5 | X | X |
| 5CNT THF | THF | MWCNTs | 5 | X | X |
| 5G THF | THF | Graphite | 5 | X | X |
| 7G THF | THF | Graphite | 7 | X | X |
| 10G THF | THF | Graphite | 10 | X | X |
| 20G THF | THF | Graphite | 20 | - | X |
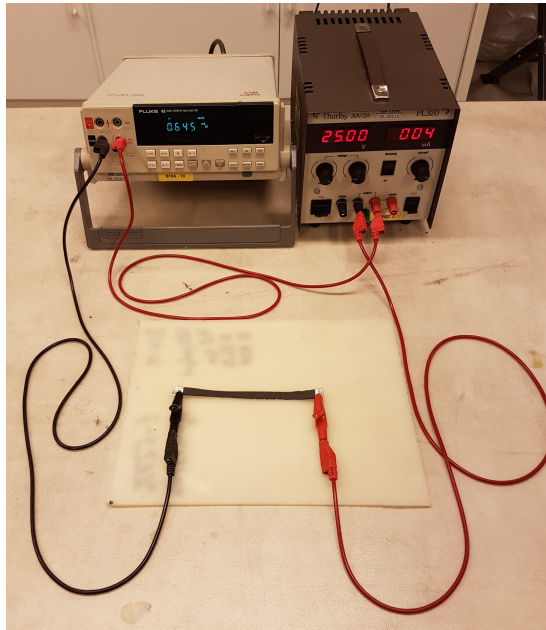
*Figure 8: Thurbly PL320 power supply and Fluke 45 multimeter used in setup for resistivity measurement.*

A 1000 cycle load-unload test to 50 MPa, or about 50% of maximum stress is conducted to investigate any loss of conductance. The test rate is set to 1.5 mm/min.

### 2.3.5 Ultrasonic imaging

A Dolphicam2 ultrasonic imaging camera was used on the CFRP-PUR composite to capture images before and after testing. The images investigated is a B-scan (Brightness scan) of the CFRP-PUR composite which is a two dimensional cross section view using a 4.5 MHz transducer adjusted for the speed of sound in CFRP at 3000 m/s.
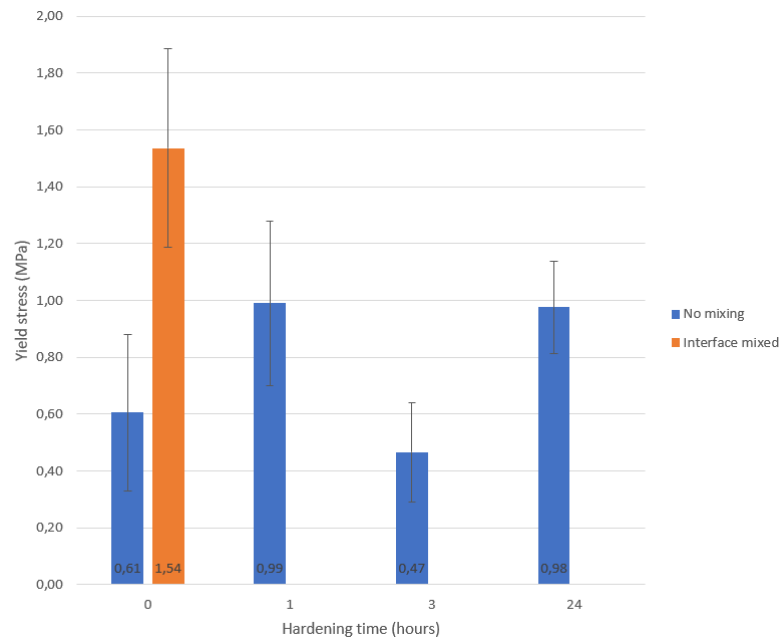
*Figure 9: Loadunload setup*

*Figure 10: Adhesion strength in correlation with PUR curing time and mixing.*

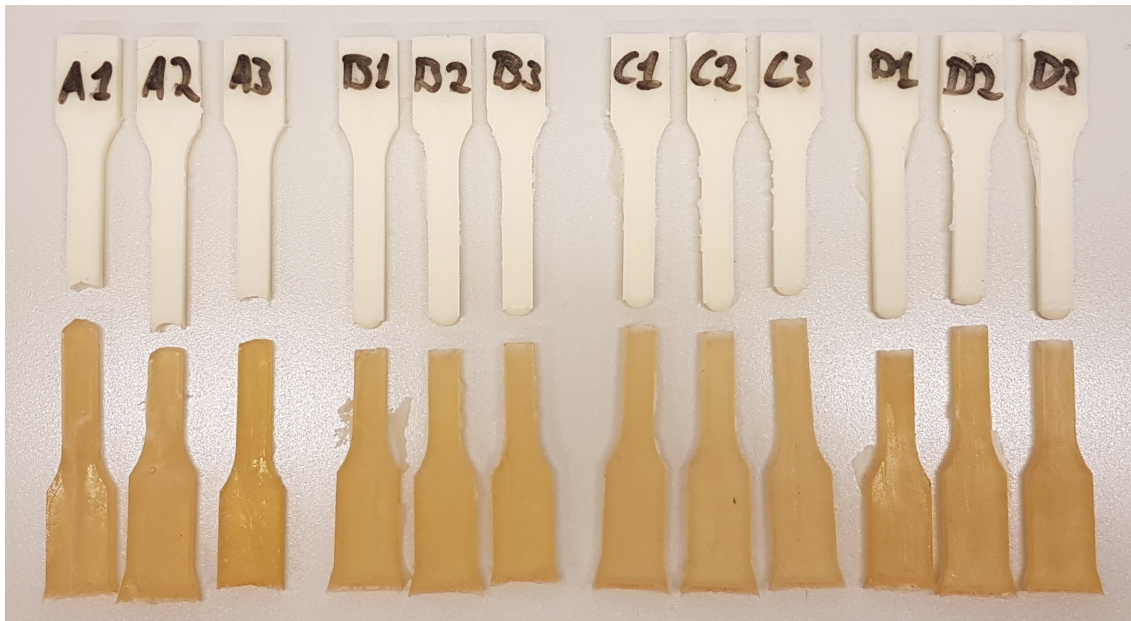# 3 Results

## 3.1 Adhesion testing

The complete list of test results from the adhesion testing can be found in appendix A. The non-mixed samples (A to D) failed in the interface, indicating that no chemical compability was achieved In addition, the results show a non-linear correlation between adhesion strength and hardening time (see figure 10). This could be caused by the change of surface roughness between the two parts of the samples (see figure 20). There was some curvature change between samples A and B.

Samples with mixed interface exhibited a higher tensile strength, as well as a failure in the new non-defined interface between the PUR-epoxy mix and the pure PUR part of the sample (see figure 10 and 12) (except for sample X3). This indicates that the bonding is achieved and that chemical bonding is stronger than the PUR material alone.

14

*Figure 11: Adhesion testing samples after results were gathered.*

## 3.2 Mechanical properties of PUR

A comparison of mechanical properties can be found in figure 14a, b and c, compairing Young's modulus, stress at strength and strain at strength respectively. The complete report of all tensile tests can be found in appendix B. Samples above 10 wt.% filler were not tested due to being too porous for the pneumatic grips, as well as being too weak for the 10 kN load cell.

It was found that the use of acetone as a solvent increased the Young's modulus and tensile stress at tensile strength, but lowered the tensile strain at tensile stress, resulting in an increased stiffness and strength of the material. The use of THF as a solvent decreased the tensile strength of the PUR, as well as lowering the Young's modulus and the tensile strain at strength. The comparison of the two solvents to a reference PUR can be found in figure 13.
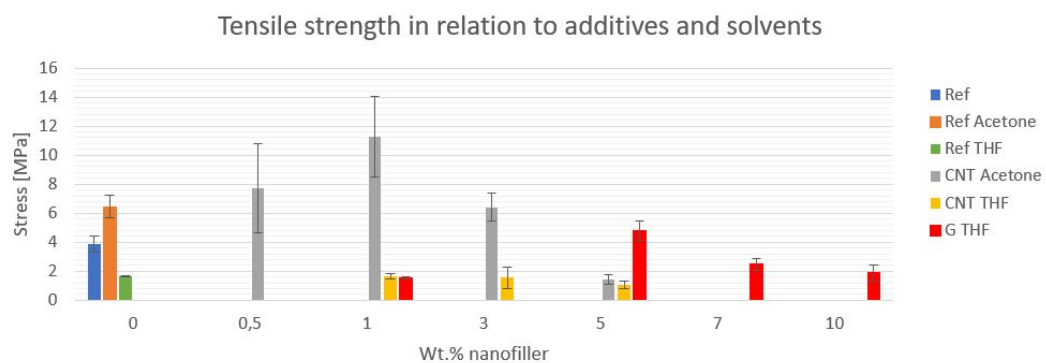
*Figure 12: Mixed interface adhesion testing samples after results were gathered.*
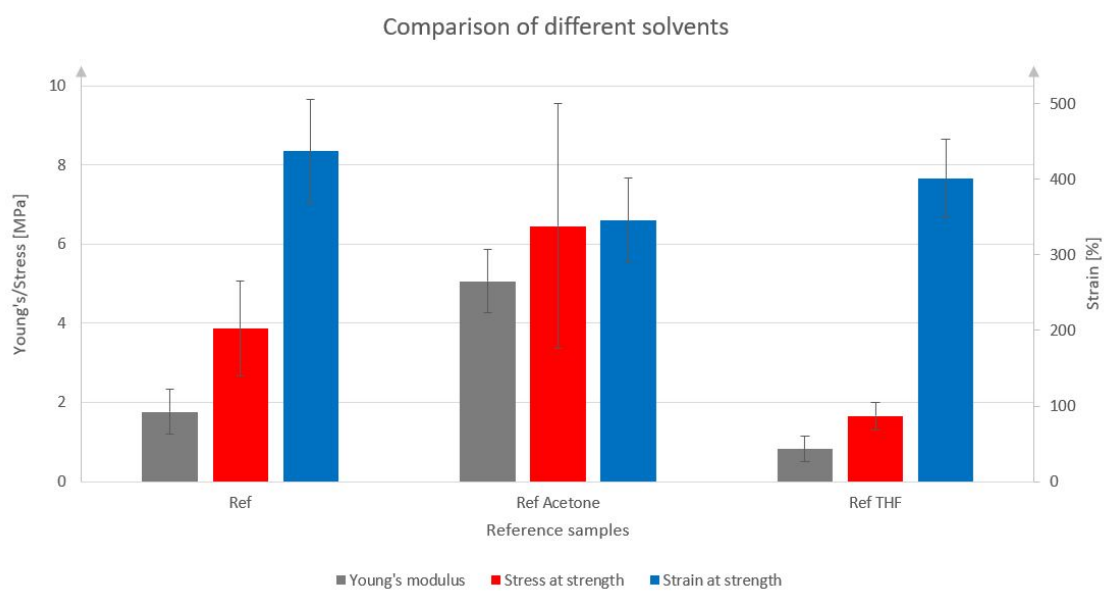
*Figure 13: Comparison of solvents used in the production of PUR electrodes. All samples are reference samples with no nanoadditives. The right vertical axis corresponds to strain (blue bar).*
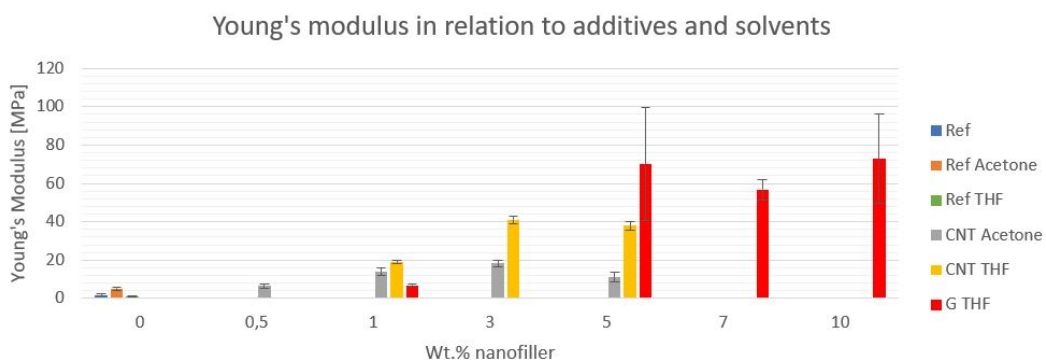
*(a) Variation in Young's modulus based on changes to solvents and additives.*



*(b) Variation in tensile stress at tensile strength based on changes to solvents and additives.*
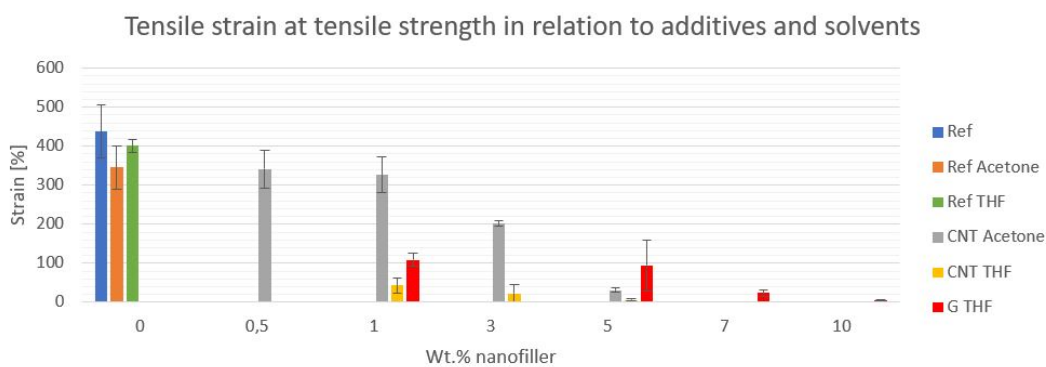


*(c) Variation in tensile strain at tensile strength based on changes to solvents and additives.*

*Figure 14: Comparison of electrodes with different solvents and nanofillers. "Ref", "Ref acetone" and "Ref THF" refers to samples without any nanoadditives.*
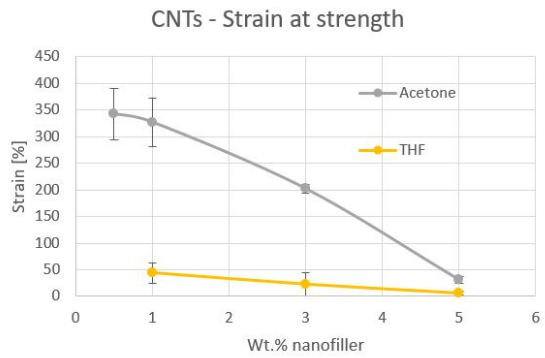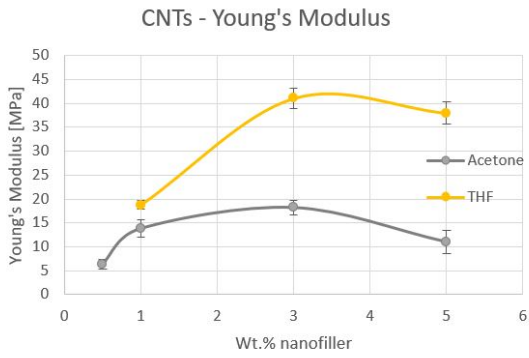
*(a) Young's modulus of electrodes with CNTs.*     *(b) Strain at strength of electrodes with CNTs.*
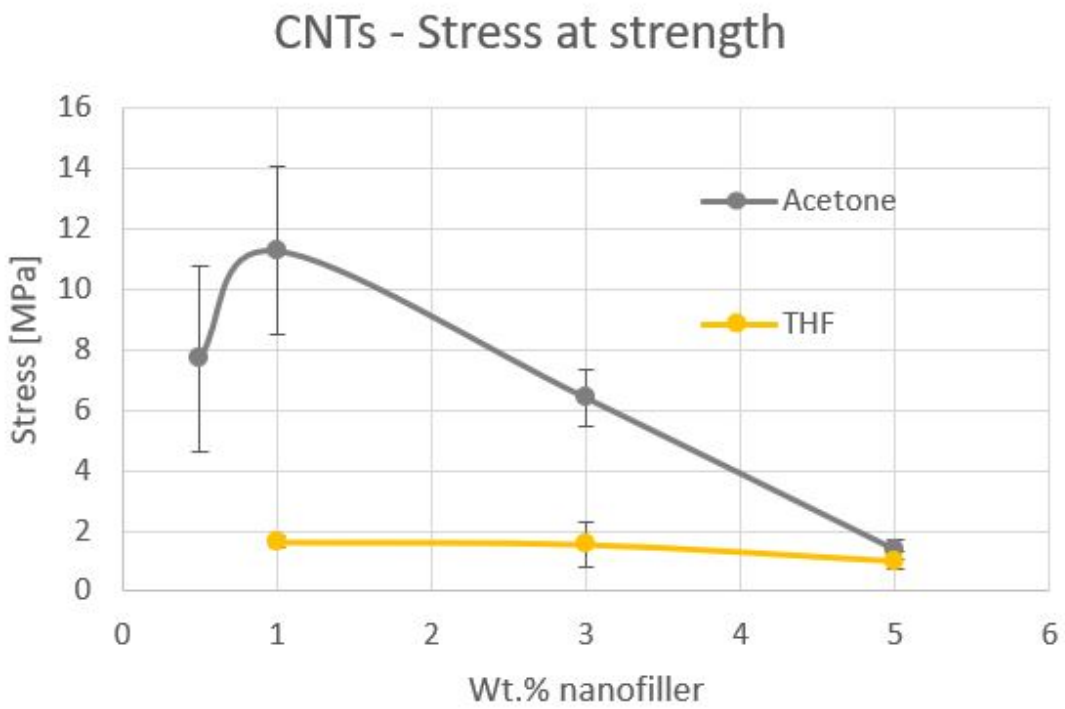


*(c) Stress at strength of electrodes with CNTs.*

*Figure 15: Mechanical properties of electrodes with CNTs.*
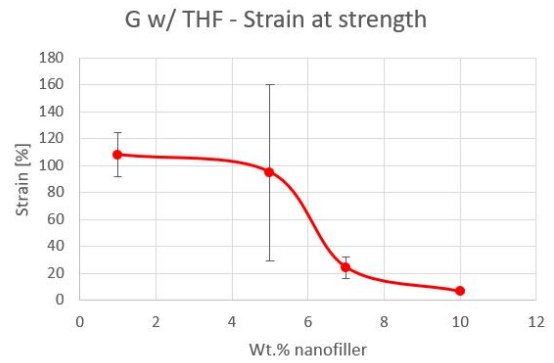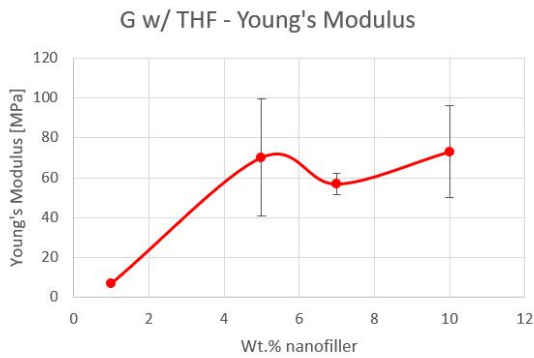
*(a) Young's modulus of electrodes with graphite that used THF as solvent.*



*(b) Strain at strength of electrodes with graphite that used THF as solvent.*



*(c) Stress at strength of electrodes with graphite that used THF as solvent.*

*Figure 16: Mechanical properties of electrodes with graphite and THF solvent.*
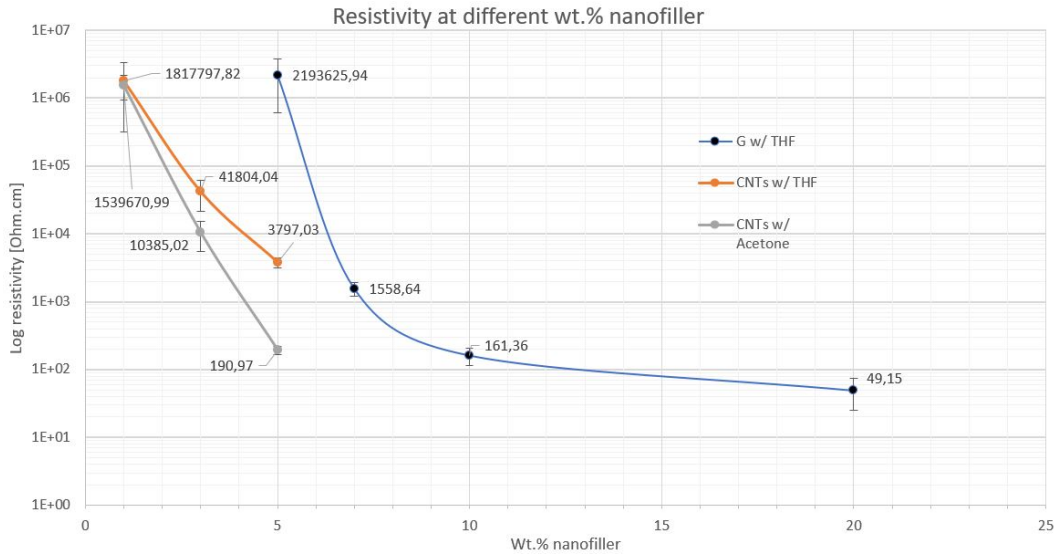
*Figure 17: Resisitivity measurements at different wt.% nanofillers.*

## 3.3   Electrical properties of PUR

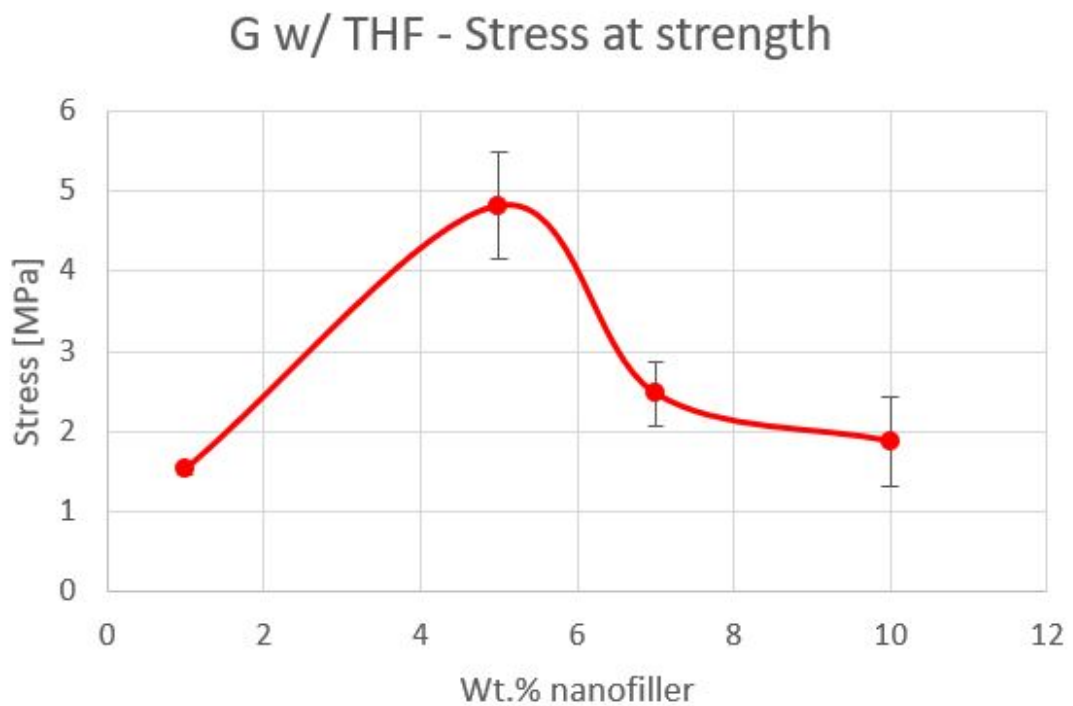The change of electrical properties in PUR when different nanoparticles and solvents are used is shown in figure 17. The electrical properties when using CNTs are better than when using graphite. This allowed for lower filler volume, having positive effects on the mechanical properties. The use of acetone as solvent proved to give lower resistivity in the samples.

## 3.4   Load-unload testing

Results show a correlation between strain and resistance. Figure 18a and b show the results from the load-unload testing. There is no apparent loss of contact in the electrodes as the lowest value of $\Delta R/R_0$ fluctuates in all load phases (figure 18a).

The results of the 1000 cycle load-unload test can be found in table 3. The change is a total of $878\,\Omega$, which is within the standard deviation during testing. This indicates no loss of contact between the electrodes and fibres.
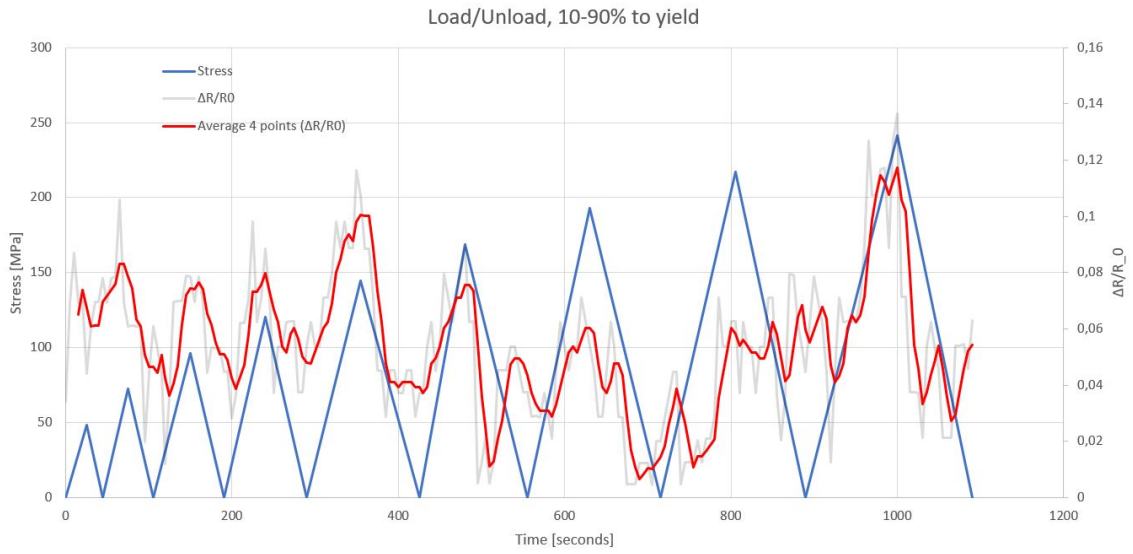
*(a) Results from load-unload test 1.*
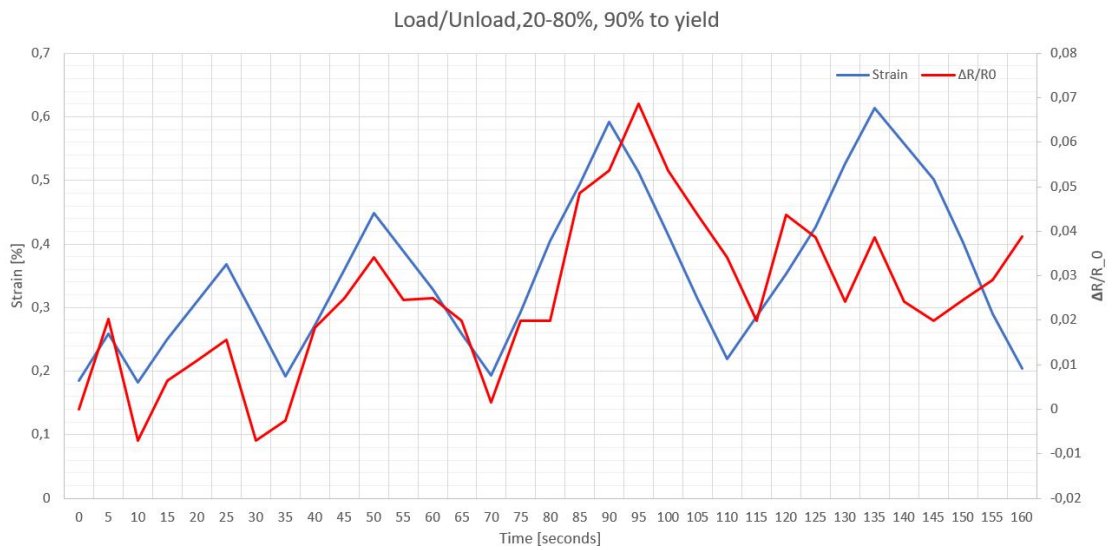


*(b) Results from load-unload test 2.*

*Figure 18: Results from load-unload testing. The blue line describes strain or stress (left vertial axis), while the red line shows the resistance in relation to the resistance with no strain (right vertial axis).*

22

*Table 3: The change of resistance during low-cycle loading*

| Cycles | Resistance |
|--------|------------|
| 0 | 159 836 $\Omega$ |
| 1000 | 160 714 $\Omega$ |

## 3.5   Ultrasonic imaging

The images taken of the electrode area of the CFRP (figure 19) show no signs of voids or significant changes to the structure. In both images the area with the electrodes show less acoustic reflection from the back wall caused by the good acoustic absorbing properties of polyurethane (Dib, Bouhedja, and Amrani 2015).



*Figure 19: Ultrasonic cross-section (b-scan) image of the interface between CFRP and PUR*

# 4 Discussion

## 4.1 The effect of sonication and solvent

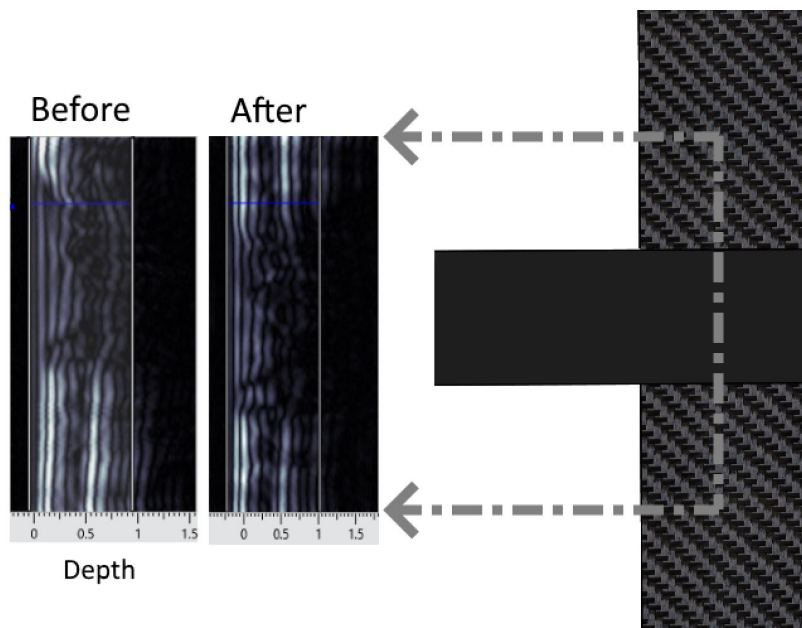It was found that the effect of sonication, type- and amount of solvent used had a significant impact on the electrical (figure 17) and mechanical (figure 13) properties of the PUR electrodes. When sonicating, the amount of solvent needed is high to ensure a good dispersion of the nanoadditives. Cheng et al. (2010) found that the effectiveness of the sonication method is dependent on many different properties such as viscosity, surface tension, molecular weight and density, but defining the effect of the sonication is highly dependent on the time spent sonicating. This is the reason the sonication was done for 30 min before adding polyol, and 30 min after. By using THF in a no-recovery distillation process is expensive, so the amount of THF that was used is minimal. This causes the viscosity to be high and the additives to adhere to the sonode, resulting in a lower-quality sonication process and therefore lower quality on the PUR electrodes.

## 4.2 Production method of polyurethane electrodes

As CNTs have a tendency to agglomerate due to Van der Waals interactions (A. Paipetis and Kostopoulos 2012). Using a solvent in the nanocomposite prepolymer solution lowers the viscosity and allows for easier mixing when using a sonicator (Pokharel et al. 2019). This causes the nanoadditives to become finely dispersed in a colloidal suspension, maximising the conductivity they provide to the PUR. This method of mixing has been proven and is common when producing polymer composites (Coleman et al. 2006; Cheng et al. 2010).

The THF proves to be a challenge to handle during long periods of sonication due to heating of the liquid and therefore increased vaporisation rate. This caused the polyol-nanofiller mix to adhere to the sonode, causing further issues when sonicating. The distillation of THF on a hotplate resulted in a wet foam-like texture. This proved difficult to

24

mix with the remaining chemicals. This consistency lead to an increase in porousity in the PUR electrodes, reflected in the results (section 3.2).

When using acetone, the amount of solvent used was greater and allowed for more consistent sonication. In combination with the mechanical changes that THF or acetone brings to the PUR without any additives (see figure 14), the electrical properties (figure 17) was also improved.

## 4.3   Production method of the CFRP-PUR composite

The method of joining electrodes and composite proved to be hard. Both parts had to be uncured, requiring timing and fidelity to align the electrodes properly. When applying the first layer of carbon fibre, a small amount of PUR permeated through (as seen in figure 6b). This PUR is mixed with epoxy and cured under pressure, limiting its permeation to other layers. Layer permeation is unwanted as it could increase the chance of a delamination due to differences in material properties between the layers, increasing the stress concentraion in this area.

## 4.4   Electrical properties of nano-enhanced polyurethane

The electical percolation threshold for CNTs in PUR is quite high due to it being an elastomer (Araby et al. 2013). To lower the required amount of CNTs needed, and therefore also the price, a combination of carbon black, graphene nanoplatelets and other cheaper additives can be added. Pokharel et al. (2019) proved that a combination of different nanofillers lowers the electrical percolation threshold, achieving a lower surface resistivity by adding 0.5 wt.% graphene nanoplatelets and CB to 1 wt.% CNTs (for a total filler content of 2 wt.%) rather than having pure 2 wt.% of CNTs. In this paper, we only measured the effect of having a single type of nanofiller for simplicity and to avoid variation in the results.

## 4.5 Mechanical properties of nano-enhanced polyurethane

The difference of mechanical properties in the reference samples is likely due to residual solvent being left in the solution after distillation. The additives increase the strength and stiffness of the material up until about 1-2 wt.%. After this point, the volume of fillers cause the PUR to become brittle, decreasing the mechanical properties. The mix of good electrical and mechanical properties provide a flexible electrode that will adhere to the carbon fibres during mechanical loading, while still conducting electricity.

## 4.6 Adhesion testing

The results gathered from the adhesion testing resulted into a worth noting pattern that does not correspond with expectations or results gathered from the paper written by Juss and Mertiny (2009). As shown in figure 20, A samples (no cure time) have a convex surface, which is the opposite of all the other samples (B to D)(cure time of 1 h or more). This is due to the density of the PUR which is lower than the density of epoxy, causing the epoxy to float when in a low-viscocity state before the curing process starts. This increases the adhesion area, effecting the adhesion testing result. In addition, the irregular texture of the interface between PUR and epoxy in the non-mixed samples could have caused the mechanical bonding to be greater. The strength of the mixed samples were on average almost 3 times as strong as the same hardening time without mixing. This proves that the mixing of epoxy-PUR interface provides a great increase in the adhesion strength.

Another proven method of testing adhesion strength is the lap shear test. This method was not used due to the difficulty introduced by the two materials to be bonded being in liquid form before curing.

26

*Figure 20: The interfacial curvature change of the adhesion testing between samples A and B.*

## 4.7    Signal from load-unload testing

The signal recieved from the load-unload testing is noisy. This could be caused by many factors, but the most dominant cause is the short gauge length between the electrodes. In addition, the PUR electrodes are not as conductive as previously achieved in other papers by Pokharel et al. (2019) and Araby et al. (2013). This caused the current to be low, resulting in a small measured change of resistance. This small change is then affected by the resolution of the multimeter, giving a noisy signal.

## 4.8    Usability in real-life application

This method of integrating electrodes in a CFRP could provide a highly durable connection without directly exposing fibres to external impact such as moisture and ultraviolet radiation.

The curing polyurethane is liquid at low (0-1) wt.% nanofillers, leading to it having to be contained during its hardening process. At higher filler content, the texture was foam-like and easier to handle. This could be utilised for in-situ preparation of samples, as the un-cured PUR stays in its moulded shape during the curing process.

For scaling these electrodes, a method of integrating in the center of the component needs to be developed. This method of having electrodes on the side of the samples causes trimming of the edge to be difficult without damaging the electrodes.

## 4.9    Further work

An important part of evaluating the usefulness of these electrodes are to look at performance after exposure to high cycle loading. As the load-unload testing showed no definite sign of interface degradation, further testing with a higher cycle count as well as a longer gauge length for more precise results is required.

A pre-fabricated and cured version that is adhered to the carbon fibres before epoxy is introduced should be tested, as it simplifies the problem of having a cure-time as well as having to be reacted at the same time as the composites epoxy. As the PUR is connected directly to the outside of the fibre strands, it should not affect the wetting process of the fibres. This method will affect the bonding between the electrodes and the composite as the chemical bonding depicted in figure 1 will not take place.

To determine the durability of the electrodes, weathering testing should be conducted to evaluate the bonding in environments involving high humidity, salinity and UV.

# 5    Conclusion

The objective of this thesis was to investigate the efficiency of using conductive polyurethane as integrated electrodes in CFRP composites for multiple applications such as strain sensing or determining structural degradation. It was found that minimum 5 wt.% of graphite

or 1 wt.% of CNT had to by added to achieve conductivity, and that a filler volume for more than 10 wt.% made the samples non-suitable for mechanical applications. The optimal solution regarding conductivity and strength was found to be 3 wt.% CNT with acetone as solvent.

The mechanical and adhesive properties were recorded using a tensile testing machine. It was found that the polyurethane electrodes have good adhesive properties when combined with epoxy in the matrix of CFRPs, and was able to bond and conduct electricity through the carbon fibres. The electrical properties achieved by adding 3 wt.% CNT proved to be good enough for utilising the gauge factor of carbon fibres.

# Acknowledgements

# References

Araby, Sherif et al. (2013). "A novel approach to electrically and thermally conductive elastomers using graphene". In: *Polymer* 54.14, pp. 3663–3670. ISSN: 0032-3861. DOI: 10.1016/j.polymer.2013.05.014.

Cheng, Qiaohuan et al. (2010). "Ultrasound-Assisted SWNTs Dispersion: Effects of Sonication Parameters and Solvent Properties". In: *The Journal of Physical Chemistry C* 114.19, pp. 8821–8827. DOI: 10.1021/jp101431h.

Coleman, Jonathan N. et al. (2006). "Small but strong: A review of the mechanical properties of carbon nanotube–polymer composites". In: *Carbon* 44.9, pp. 1624–1652. ISSN: 0008-6223. DOI: 10.1016/j.carbon.2006.02.038.

Dib, Lyes, S Bouhedja, and Hamza Amrani (2015). "Mechanical Parameters Effects on Acoustic Absorption at Polymer Foam". In: *Advances in Materials Science and Engineering* 2015. DOI: 10.1155/2015/896035.

Fried, JR (1997). *Polymer Science and Technology*. Prentice Hall PTR, Englewood Cliffs.

Fukuda, Hiroshi (1994). "Processing of carbon fiber reinforced plastics by means of Joule heating". In: *Advanced Composite Materials* 3.3, pp. 153–161.

Grammatikos, S.A. and A.S. Paipetis (2012). "On the electrical properties of multi scale reinforced composites for damage accumulation monitoring". English. In: *Compos., B, Eng. (UK)* 43.6, pp. 2687–96. ISSN: 1359-8368.

Joo, Sung-Jun et al. (2017). "In situ fabrication of copper electrodes on carbon-fiber-reinforced polymer (CFRP) for damage monitoring by printing and flash light sintering". In: *Composites Science and Technology* 142, pp. 189–197. ISSN: 0266-3538. DOI: https://doi.org/10.1016/j.compscitech.2017.02.011.

Juss, K. and P. Mertiny (2009). "Assessment of adhesion between polyurethane liner and epoxy based substrate: Methodology and experiment". In: *Polymer Testing* 28.7, pp. 764–769. ISSN: 0142-9418.

Karl, Schulte and Ch Baron (1989). "Load and Failure Analyses of CFRP Laminates by Means of Electrical Resistivity Measurement". In: *Composites Science and Technology* 36, pp. 63–76. DOI: 10.1016/0266-3538(89)90016-X.

Narayana, K. Jagath and Ramesh Gupta Burela (2018). "A review of recent research on multifunctional composite materials and structures with their applications". In: *Materials Today: Proceedings* 5.2, Part 1. 7th International Conference of Materials Processing and Characterization, March 17-19, 2017, pp. 5580–5590. ISSN: 2214-7853. DOI: https://doi.org/10.1016/j.matpr.2017.12.149. URL: http://www.sciencedirect.com/science/article/pii/S2214785317331280.

Paipetis, A. and V. Kostopoulos (2012). *Carbon Nanotube Enhanced Aerospace Composite Materials: A New Generation of Multifunctional Hybrid Structural Composites*. Solid Mechanics and Its Applications. Springer Netherlands. ISBN: 9789400742468.

Pokharel, Pashupati et al. (2019). "A hierarchical approach for creating electrically conductive network structure in polyurethane nanocomposites using a hybrid of graphene nanoplatelets, carbon black and multi-walled carbon nanotubes". English. In: *Composites Part B: Engineering* 161, pp. 169–182. ISSN: 13598368.

Saunders, J.H. and K.C. Frisch (1964). *Polyurethanes: chemistry and technology, part II: Technology*. Interscience Publishers, New York.

Urbanski, J et al. (1977). *Handbook of analysis of synthetic polymers and plastics*. Ellis Horwood Limited, Chichester.

Wang, Xiaojun and D.D.L. Chung (1997). "Sensing delamination in a carbon fiber polymer-matrix composite during fatigue by electrical resistance measurement". In: *Polym. Compos. (USA)* 18.6, pp. 692–700. ISSN: 0272-8397.

Wang, Xiaojun, Xuli Fu, and Deborah Chung (1999). "Strain Sensing Using Carbon Fiber". In: *Journal of Materials Research - J MATER RES* 14, pp. 790–802. DOI: 10.1557/JMR.1999.0105.

Xi, Xiang and D.D.L. Chung (2019). "Piezoelectric and piezoresistive behavior of unmodified carbon fiber". English. In: *Carbon* 145, pp. 452–461. ISSN: 00086223. URL: http://dx.doi.org/10.1016/j.carbon.2019.01.044.

Yao, Xudan, Stephen C. Hawkins, and Brian G. Falzon (2018). "An advanced anti-icing/de-icing system utilizing highly aligned carbon nanotube webs". English. In: *Carbon* 136, pp. 130–138. ISSN: 00086223.

# Appendix

# A  Results from adhesion testing

| ID | Curing time [h] | Yield stress [MPa] | Failure method |
|---|---|---|---|
| A1 | | 0.89 | Interfacial failure |
| A2 | 0 | 0.59 | Interfacial failure |
| A3 | | 0.34 | Interfacial failure |
| Average | | 0.61 | |
| SD | | 0.224 | |
| B1 | | 0.71 | Interfacial failure |
| B2 | 1 | 1.29 | Interfacial failure |
| B3 | | 0.97 | Interfacial failure |
| Average | | 0.99 | |
| SD | | 0.291 | |
| C1 | | 0.53 | Interfacial failure |
| C2 | 3 | 0.60 | Interfacial failure |
| C3 | | 0.27 | Interfacial failure |
| Average | | 0.47 | |
| SD | | 0.174 | |
| D1 | | 0.95 | Interfacial failure |
| D2 | 24 | 0.83 | Interfacial failure |
| D3 | | 1.15 | Interfacial failure |
| Average | | 0.98 | |
| SD | | 0.162 | |
| X1 | | 1.35 | PUR failure above mixed zone |
| X2 | 0 | 1.94 | PUR failure above mixed zone |
| X3 | | 1.32 | Interfacial failure |
| Average | | 1.54 | |
| SD | | 0.350 | |

Tension testing based on ISO 527-2.

## Specimen 1 to 4
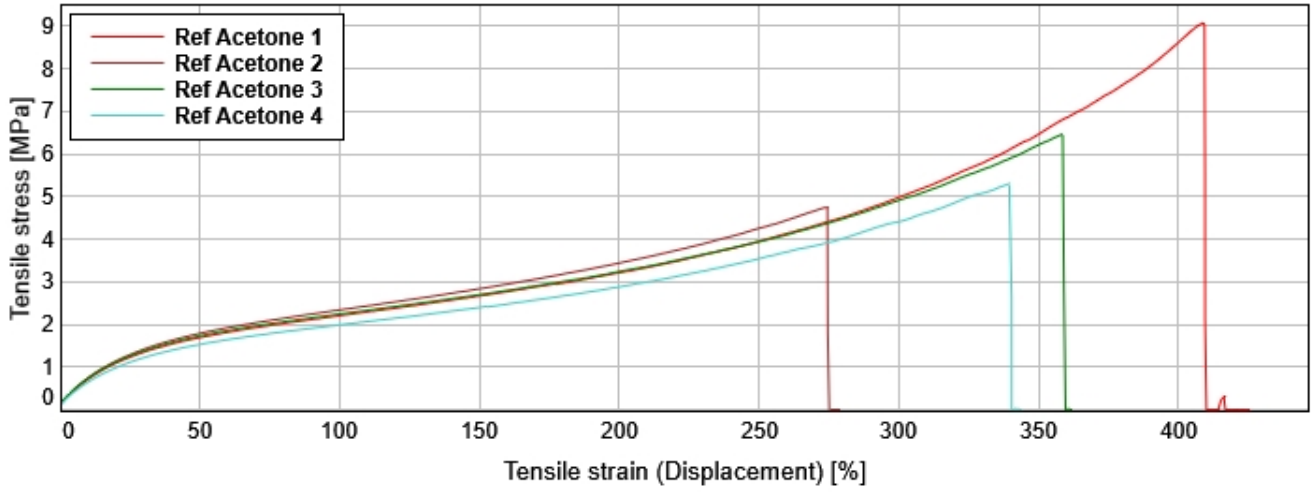


## Specimen 5 to 8
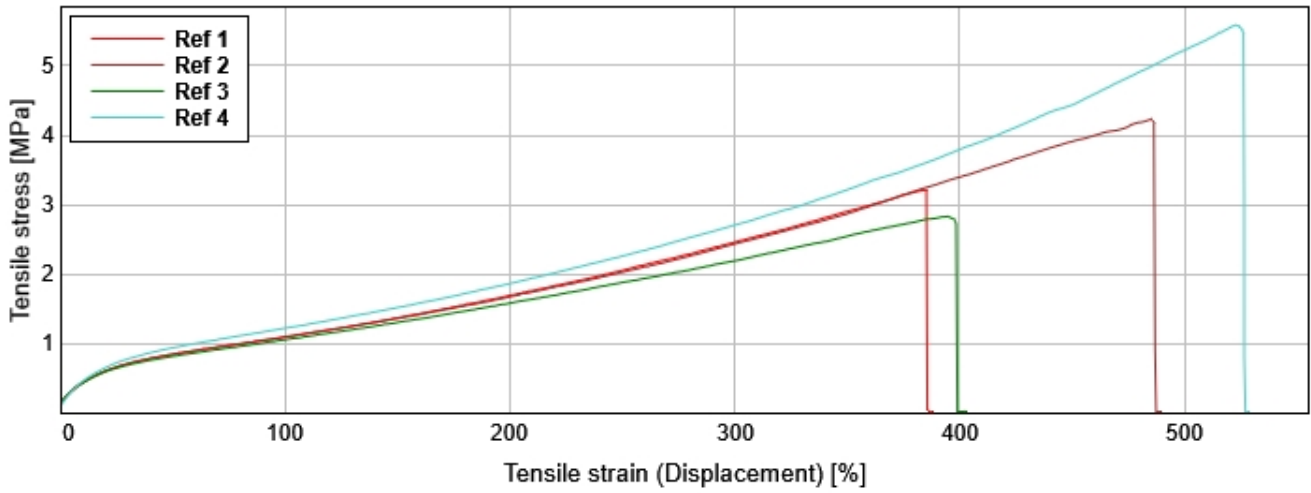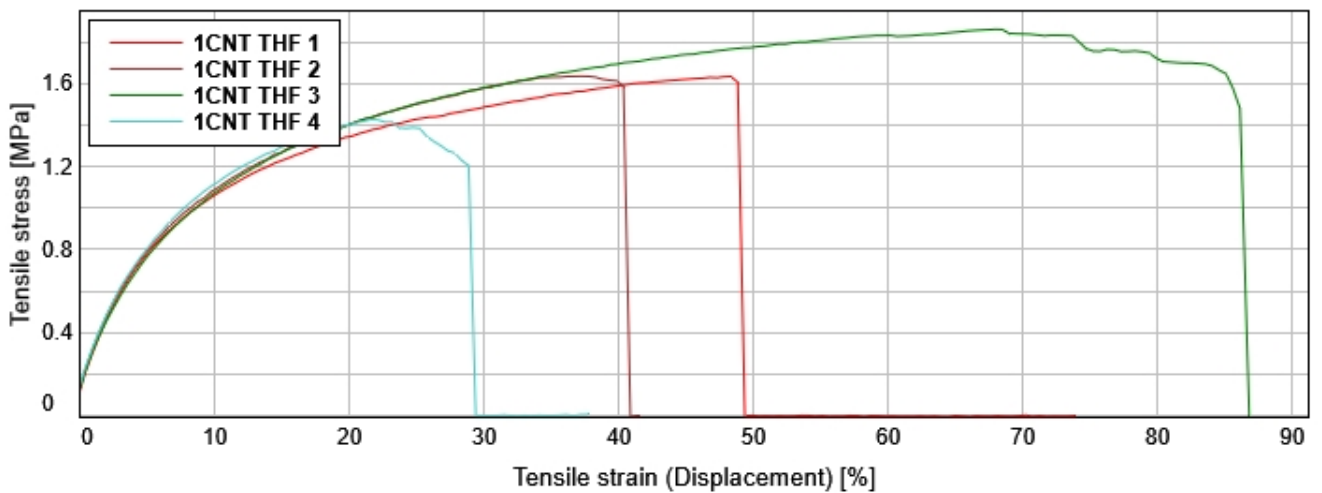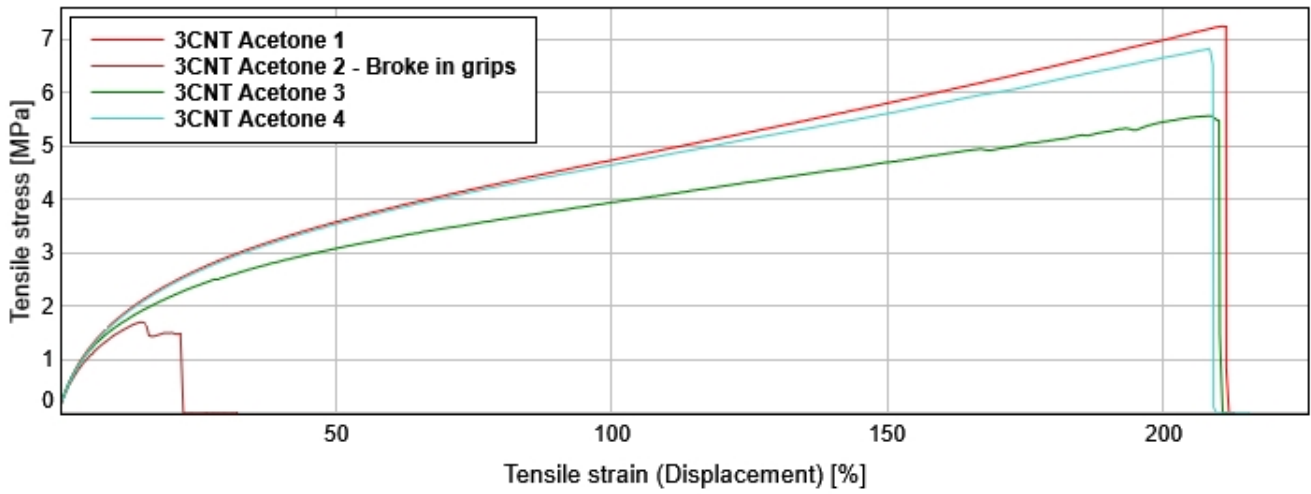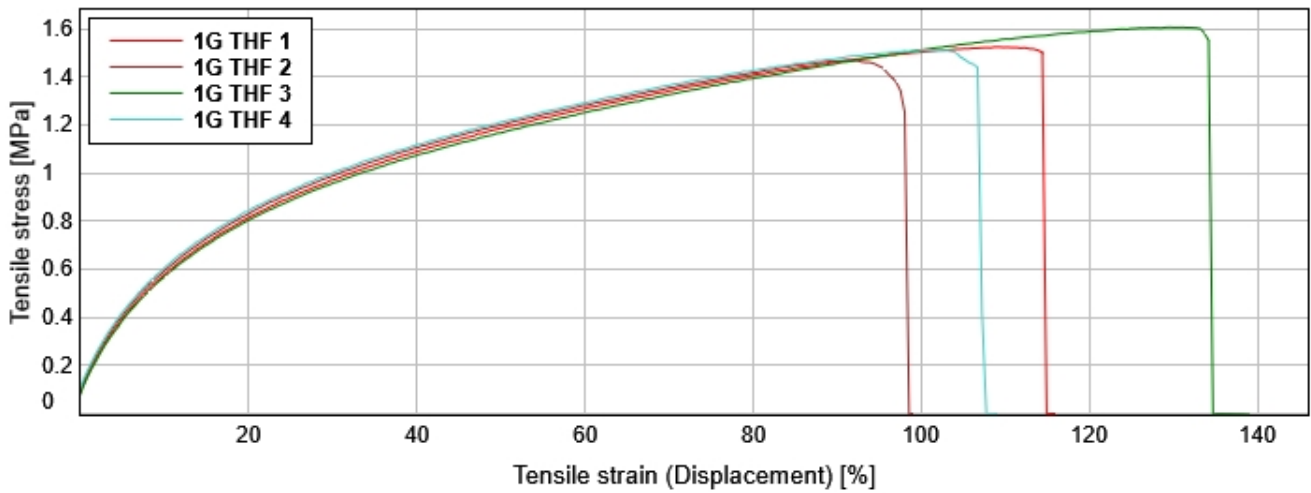
## Specimen 9 to 12
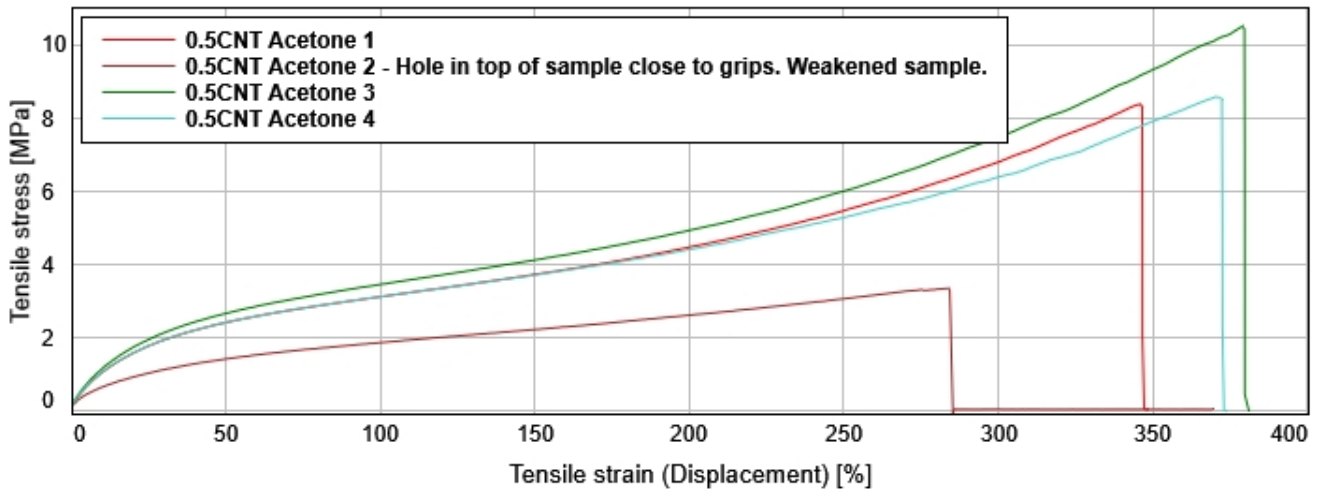


## Specimen 13 to 16
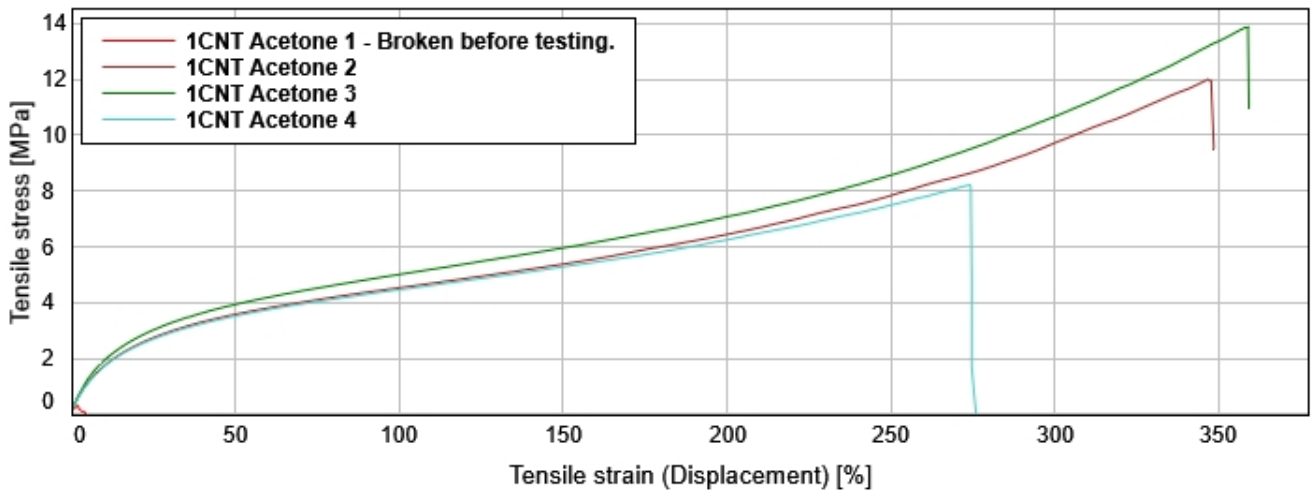


## Specimen 17 to 20

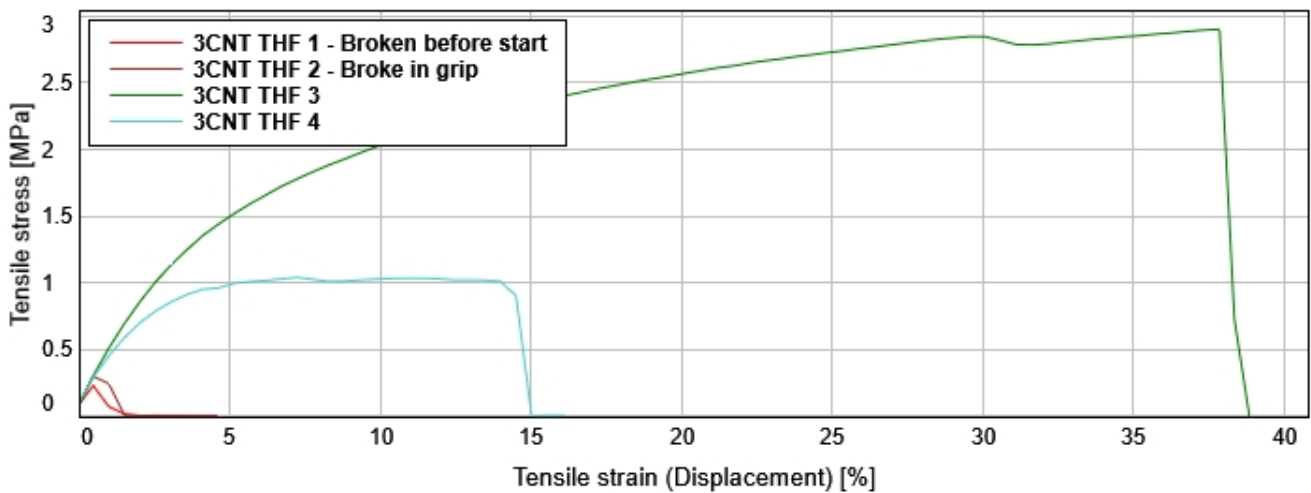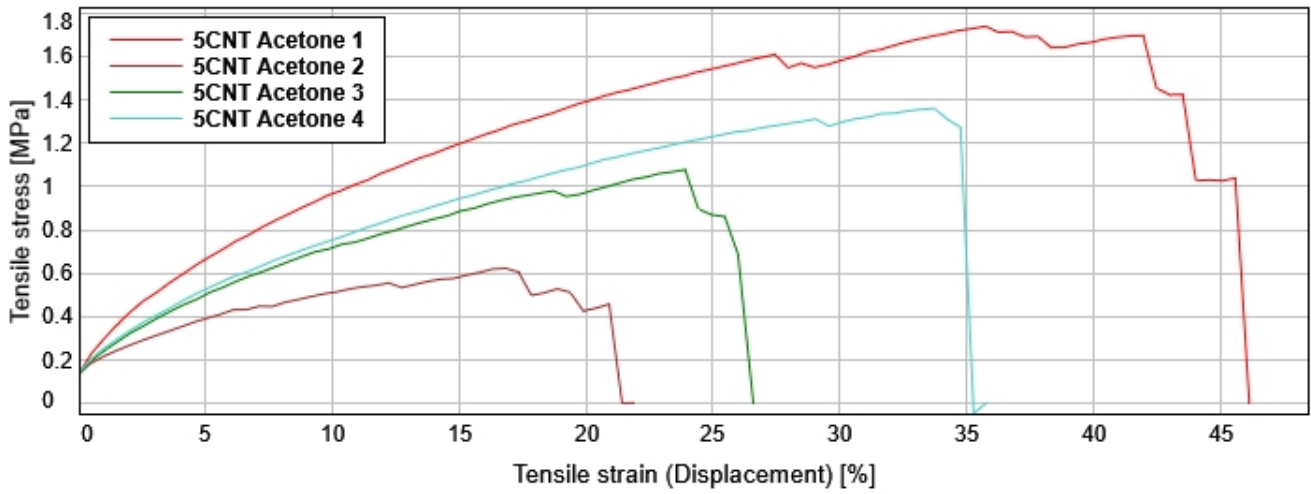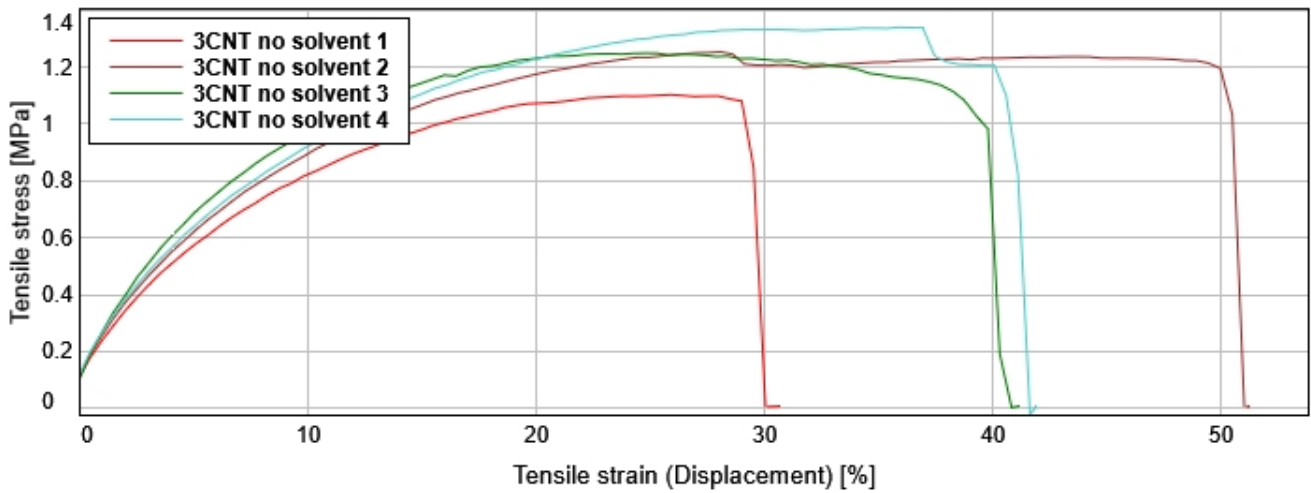## Specimen 21 to 24
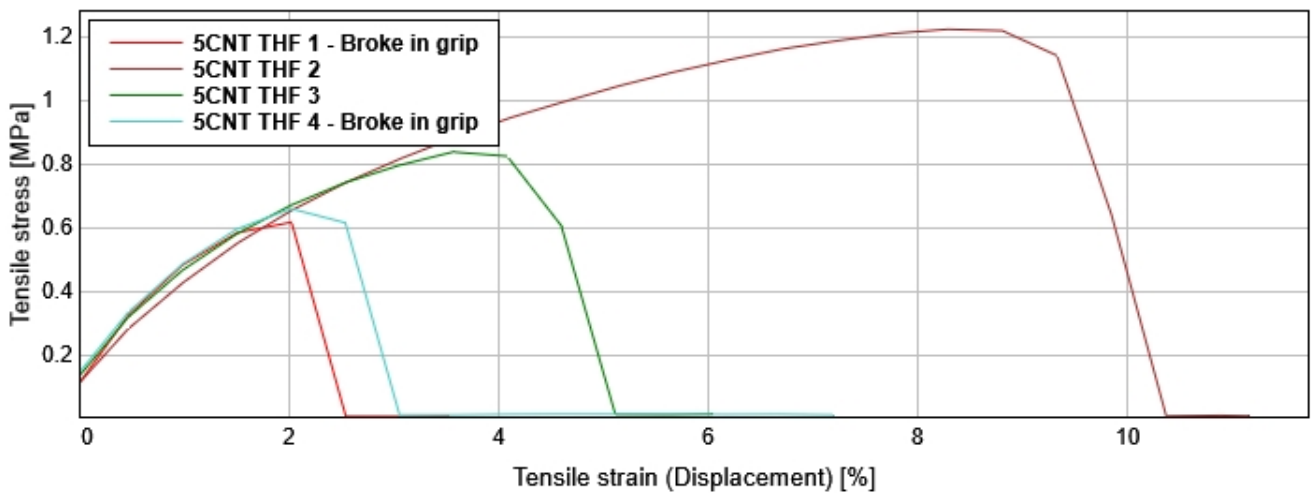


## Specimen 25 to 28



## Specimen 29 to 32

**NTNU**

## Specimen 33 to 36



## Specimen 37 to 40



## Specimen 41 to 44

**NTNU**

### Specimen 45 to 48
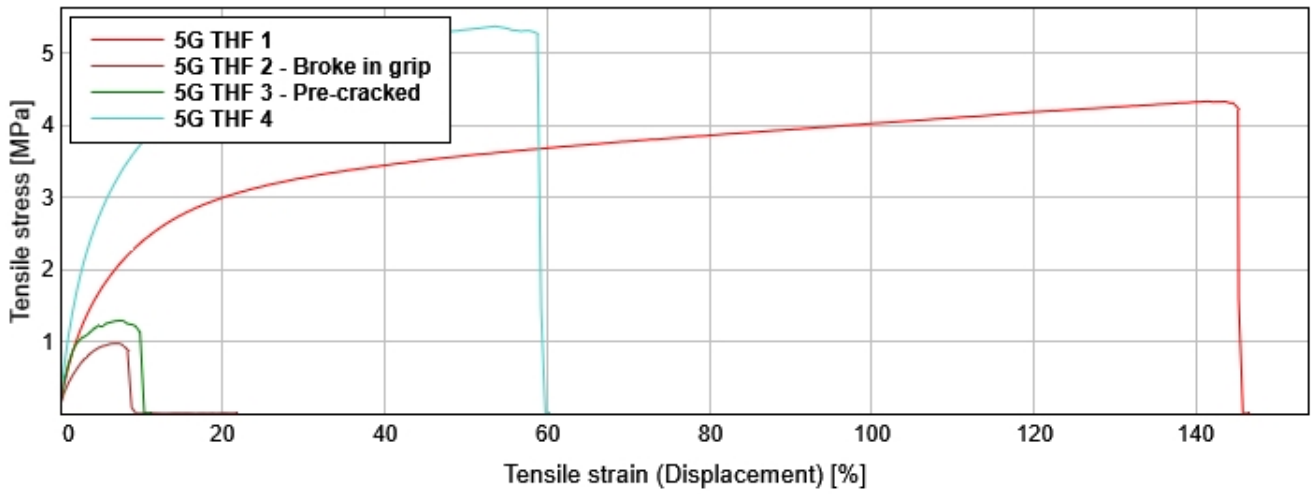


### Specimen 49 to 52
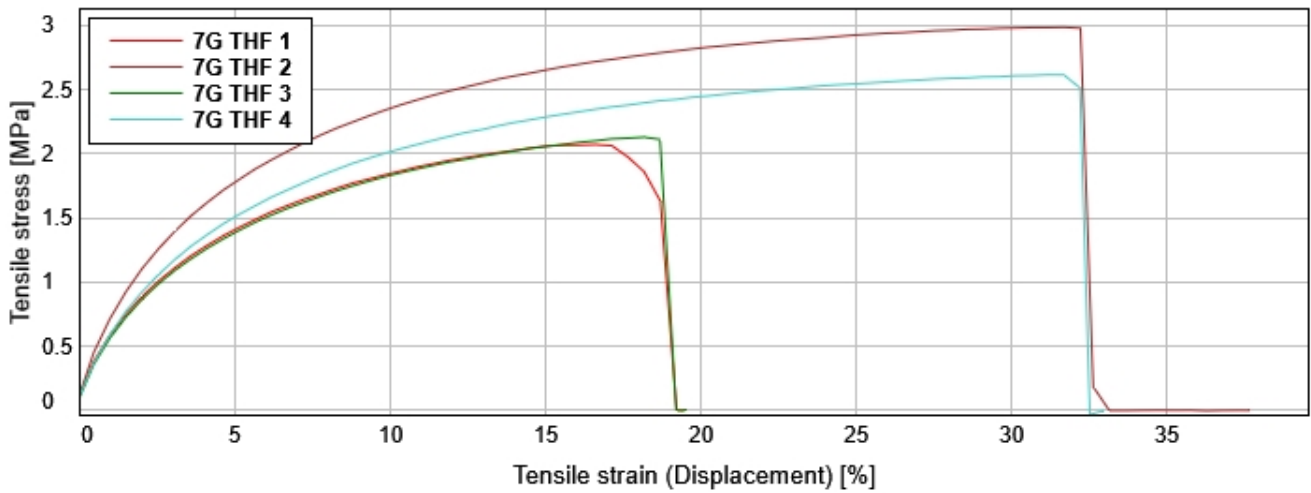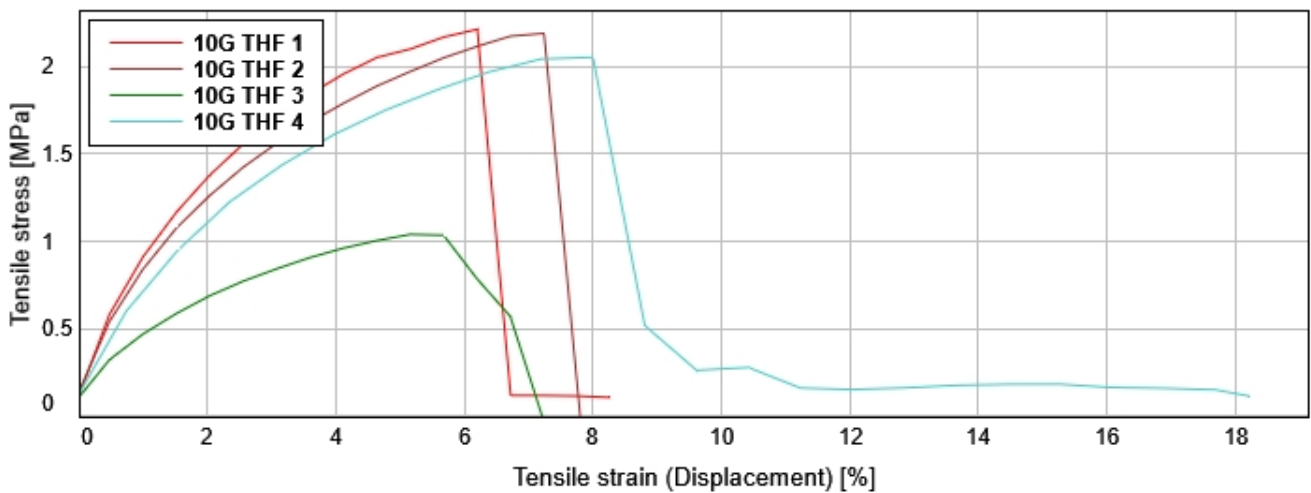


### Specimen 53 to 56

Specimen 57 to 60
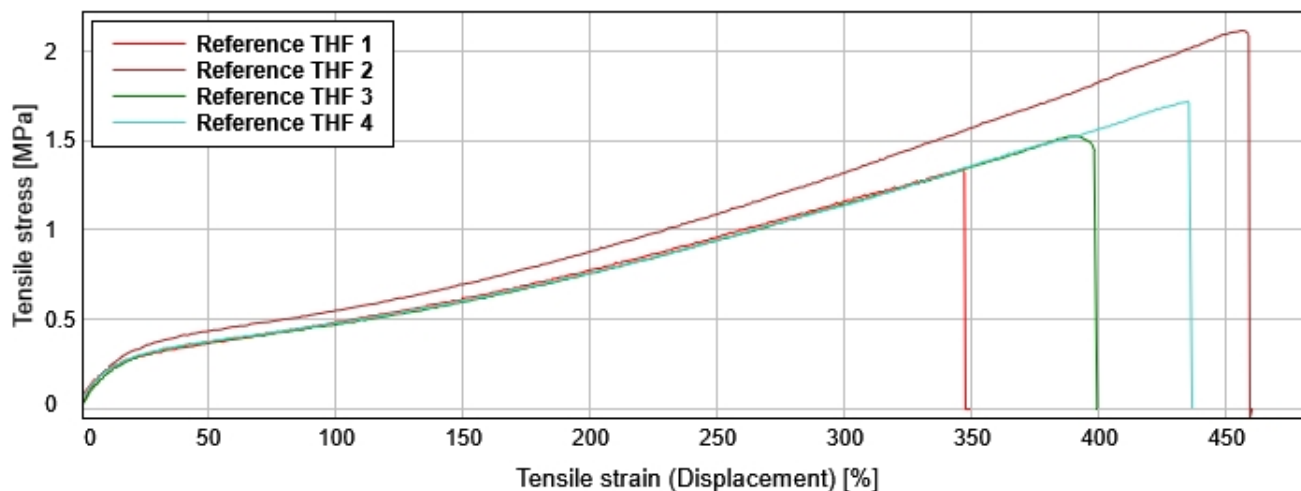
| | Specimen label ▲ | Specimen note 1 | Modulus (Automatic Young's) [MPa] | Tensile stress at Tensile strength [MPa] | Tensile strain (Displacement) at Tensile strength [%] | Area [mm^2] |
|---|---|---|---|---|---|---|
| **Specimen note 1: 0.5 wt.% CNT (Number of specimens: 4)** | | | | | | |
| 9 | 0.5CNT Acetone 1 | 0.5 wt.% CNT | 7.01 | 8.39 | 346.07 | 8.14 |
| 10 | 0.5CNT Acetone 2 - Hole in top of sample close to grips. Weakened sample. | 0.5 wt.% CNT | 4.97 | 3.29 | 272.36 | 7.31 |
| 11 | 0.5CNT Acetone 3 | 0.5 wt.% CNT | 6.86 | 10.52 | 379.12 | 7.67 |
| 12 | 0.5CNT Acetone 4 | 0.5 wt.% CNT | 6.82 | 8.61 | 370.78 | 8.21 |

| | Specimen label ▲ | Specimen note 1 | Modulus (Automatic Young's) [MPa] | Tensile stress at Tensile strength [MPa] | Tensile strain (Displacement) at Tensile strength [%] | Area [mm^2] |
|---|---|---|---|---|---|---|
| **Specimen note 1: 1 wt.% (Number of specimens: 12)** | | | | | | |
| 13 🚫 | 1CNT Acetone 1 - Broken before testing. | 1 wt.% | ----- | 0.31 | 2.03 | 9.00 |
| 14 | 1CNT Acetone 2 | 1 wt.% | 12.41 | 12.02 | 347.13 | 9.54 |
| 15 | 1CNT Acetone 3 | 1 wt.% | 13.14 | 13.86 | 358.88 | 8.56 |
| 16 | 1CNT Acetone 4 | 1 wt.% | 15.91 | 8.22 | 274.34 | 7.93 |
| 17 | 1CNT THF 1 | 1 wt.% | 18.53 | 1.63 | 48.34 | 9.70 |
| 18 | 1CNT THF 2 | 1 wt.% | 18.69 | 1.64 | 37.27 | 8.21 |
| 19 | 1CNT THF 3 | 1 wt.% | 17.95 | 1.86 | 67.94 | 8.71 |
| 20 | 1CNT THF 4 | 1 wt.% | 19.98 | 1.43 | 21.67 | 7.96 |
| 25 | 1G THF 1 | 1 wt.% | 6.83 | 1.52 | 109.46 | 14.09 |
| 26 | 1G THF 2 | 1 wt.% | 7.22 | 1.47 | 91.35 | 12.67 |
| 27 | 1G THF 3 | 1 wt.% | 6.55 | 1.60 | 130.18 | 15.10 |
| 28 | 1G THF 4 | 1 wt.% | 7.25 | 1.51 | 101.28 | 11.03 |

| | Specimen label ▲ | Specimen note 1 | Modulus (Automatic Young's) [MPa] | Tensile stress at Tensile strength [MPa] | Tensile strain (Displacement) at Tensile strength [%] | Area [mm^2] |
|---|---|---|---|---|---|---|
| Specimen note 1: 10 wt.% G, THF (Number of specimens: 4) |
| 53 | 10G THF 1 | 10 wt.% G, THF | 97.45 | 2.21 | 6.20 | 8.08 |
| 54 | 10G THF 2 | 10 wt.% G, THF | 84.80 | 2.19 | 7.24 | 6.95 |
| 55 | 10G THF 3 | 10 wt.% G, THF | 45.14 | 1.04 | 5.16 | 8.85 |
| 56 | 10G THF 4 | 10 wt.% G, THF | 64.15 | 2.05 | 8.00 | 7.28 |

| | Specimen label ▲ | Specimen note 1 | Modulus (Automatic Young's) [MPa] | Tensile stress at Tensile strength [MPa] | Tensile strain (Displacement) at Tensile strength [%] | Area [mm^2] |
|---|---|---|---|---|---|---|
| Specimen note 1: 3 wt.% (Number of specimens: 12) |
| 21 | 3CNT Acetone 1 | 3 wt.% | 17.20 | 7.25 | 210.89 | 8.11 |
| 22 🚫 | 3CNT Acetone 2 - Broke in grips | 3 wt.% | 26.69 | 1.71 | 14.53 | 7.94 |
| 23 | 3CNT Acetone 3 | 3 wt.% | 20.04 | 5.41 | 198.22 | 6.42 |
| 24 | 3CNT Acetone 4 | 3 wt.% | 17.36 | 6.60 | 197.06 | 7.94 |
| 37 | 3CNT no solvent 1 | 3 wt.% | 12.19 | 1.10 | 25.89 | 9.39 |
| 38 | 3CNT no solvent 2 | 3 wt.% | 13.55 | 1.24 | 43.70 | 9.71 |
| 39 | 3CNT no solvent 3 | 3 wt.% | 16.78 | 1.25 | 25.30 | 9.53 |
| 40 | 3CNT no solvent 4 | 3 wt.% | 13.96 | 1.33 | 28.60 | 9.25 |
| 29 🚫 | 3CNT THF 1 - Broken before start | 3 wt.% | ----- | 0.23 | 0.47 | 11.03 |
| 30 🚫 | 3CNT THF 2 - Broke in grip | 3 wt.% | ----- | 0.30 | 0.47 | 10.80 |
| 31 | 3CNT THF 3 | 3 wt.% | 42.47 | 2.90 | 37.87 | 11.69 |
| 32 | 3CNT THF 4 | 3 wt.% | 39.60 | 1.04 | 7.23 | 9.49 |

| | Specimen label ▲ | Specimen note 1 | Modulus (Automatic Young's) [MPa] | Tensile stress at Tensile strength [MPa] | Tensile strain (Displacement) at Tensile strength [%] | Area [mm^2] |
|---|---|---|---|---|---|---|
| Specimen note 1: 5 wt.% (Number of specimens: 12) |
| 33 | 5CNT Acetone 1 | 5 wt.% | 13.88 | 1.74 | 35.75 | 7.01 |
| 34 🚫 | 5CNT Acetone 2 | 5 wt.% | 7.83 | 0.62 | 16.82 | 6.83 |
| 35 | 5CNT Acetone 3 | 5 wt.% | 9.86 | 1.08 | 23.91 | 7.34 |
| 36 | 5CNT Acetone 4 | 5 wt.% | 9.47 | 1.36 | 33.73 | 6.90 |
| 41 🚫 | 5CNT THF 1 - Broke in grip | 5 wt.% | ----- | 0.62 | 2.03 | 8.81 |
| 42 | 5CNT THF 2 | 5 wt.% | 36.31 | 1.22 | 8.28 | 8.78 |
| 43 | 5CNT THF 3 | 5 wt.% | 39.65 | 0.84 | 3.57 | 7.23 |
| 44 🚫 | 5CNT THF 4 - Broke in grip | 5 wt.% | ----- | 0.66 | 2.02 | 6.74 |
| 45 | 5G THF 1 | 5 wt.% | 49.29 | 4.34 | 141.33 | 9.77 |
| 46 🚫 | 5G THF 2 - Broke in grip | 5 wt.% | 36.11 | 0.97 | 7.24 | 8.63 |

NTNU

| | | Specimen label ▲ | Specimen note 1 | Modulus (Automatic Young's) [MPa] | Tensile stress at Tensile strength [MPa] | Tensile strain (Displacement) at Tensile strength [%] | Area [mm^2] |
|---|---|---|---|---|---|---|---|
| Specimen note 1: 5 wt.% (Number of specimens: 12) | | | | | | | |
| 47 | 🚫 | 5G THF 3 - Pre-cracked | 5 wt.% | 69.91 | 1.29 | 7.24 | 8.05 |
| 48 | | 5G THF 4 | 5 wt.% | 90.78 | 5.29 | 46.83 | 6.66 |

| | Specimen label ▲ | Specimen note 1 | Modulus (Automatic Young's) [MPa] | Tensile stress at Tensile strength [MPa] | Tensile strain (Displacement) at Tensile strength [%] | Area [mm^2] |
|---|---|---|---|---|---|---|
| Specimen note 1: 7 wt.% G (Number of specimens: 4) | | | | | | |
| 49 | 7G THF 1 | 7 wt.% G | 58.11 | 2.07 | 16.62 | 8.89 |
| 50 | 7G THF 2 | 7 wt.% G | 60.99 | 2.98 | 31.69 | 9.01 |
| 51 | 7G THF 3 | 7 wt.% G | 56.39 | 2.13 | 18.17 | 10.77 |
| 52 | 7G THF 4 | 7 wt.% G | 49.20 | 2.61 | 31.16 | 9.84 |

| | Specimen label ▲ | Specimen note 1 | Modulus (Automatic Young's) [MPa] | Tensile stress at Tensile strength [MPa] | Tensile strain (Displacement) at Tensile strength [%] | Area [mm^2] |
|---|---|---|---|---|---|---|
| Specimen note 1: No additives (Number of specimens: 12) | | | | | | |
| 5 | Ref 1 | No additives | 2.19 | 3.12 | 373.38 | 7.96 |
| 6 | Ref 2 | No additives | 1.04 | 4.12 | 474.54 | 7.78 |
| 7 | Ref 3 | No additives | 2.23 | 2.79 | 386.13 | 7.30 |
| 8 | Ref 4 | No additives | 1.57 | 5.45 | 514.38 | 10.99 |
| 1 | Ref Acetone 1 | No additives | 5.23 | 9.07 | 408.87 | 7.56 |
| 2 | Ref Acetone 2 | No additives | 5.85 | 4.75 | 274.47 | 8.66 |
| 3 | Ref Acetone 3 | No additives | 4.60 | 6.47 | 358.65 | 7.36 |
| 4 | Ref Acetone 4 | No additives | 4.31 | 5.31 | 340.06 | 9.48 |
| 57 | Reference THF 1 | No additives | 0.39 | 1.30 | 335.80 | 7.03 |
| 58 | Reference THF 2 | No additives | 0.93 | 2.12 | 456.13 | 6.67 |
| 59 | Reference THF 3 | No additives | 1.14 | 1.53 | 388.54 | 6.79 |
| 60 | Reference THF 4 | No additives | 0.83 | 1.68 | 423.49 | 7.20 |